Research Square

Preprints are preliminary reports that have not undergone peer review.
They should not be considered conclusive, used to inform clinical practice,
or referenced by the media as validated information.

A dual-route model of facial trait impressions: Dissociating the perceptual and conceptual components

Amber X. Chen
University of California, Santa Barbara https://orcid.org/0000-0003-3359-9075
Caixia Liu
Shenzhen University
Shangcheng Zhao
University of California, Santa Barbara https://orcid.org/0000-0001-8878-736X
Ava Ma de Sousa
University of California, Santa Barbara https://orcid.org/0000-0001-7636-5047
Xiaozhe Peng
Shenzhen University https://orcid.org/0000-0001-5019-3101
Hongbo Yu
hongbo.yu@psych.ucsb.edu
University of California Santa Barbara https://orcid.org/0000-0002-3384-7772

Research Article

Keywords: facial trait impressions, person perception, conceptual knowledge, familiarity, representational similarity analysis, social cognition

Posted Date: September 15th, 2026

DOI: https://doi.org/10.21203/rs.3.rs-11026088/v1

License: This work is licensed under a Creative Commons Attribution 4.0 International License.
Read Full License

Additional Declarations: The authors declare no competing interests.

Note: This preprint has not been peer reviewed

A dual-route model of facial trait impressions: Dissociating the perceptual and conceptual components

Amber X. Chen[1], Caixia Liu[2], Shangcheng Zhao[1], Ava Q. Ma de Sousa[1], Xiaozhe Peng[2], Hongbo Yu[1]

[1] Department of Psychological and Brain Sciences, University of California Santa Barbara, Santa Barbara, CA 93106, USA

[2] School of Psychology, Shenzhen University, Shenzhen, 518060, P.R. China

Amber X. Chen – ORCID: 0000-0003-3359-9075

Shangcheng Zhao – ORCID: 0000-0001-8878-736X

Ava Q. Ma de Sousa– ORCID: 0000-0001-7636-5047

Hongbo Yu– ORCID: 0000-0002-3384-7772

Correspondence should be addressed

Hongbo Yu, Ph.D.

Department of Psychological and Brain Sciences,

University of California Santa Barbara,

Santa Barbara, CA 93106, USA

Email: hongbo.yu@psych.ucsb.edu

Or

Xiaozhe Peng, Ph.D.

School of Psychology,

Shenzhen University,

Shenzhen, 518060, P. R. China,

Email: pengxz@szu.edu.cn

Abstract

People form trait impressions from both facial appearance and knowledge about targets. We tested a dual-route framework in which visual and semantic information jointly contribute to impressions. Across two celebrity-impression datasets comprising 415 U.S. and 327 Chinese participants, we constructed visual representational spaces from face-recognition model embeddings and semantic spaces from embeddings of encyclopedic descriptions. We tested whether behavioral trait impressions tracked these spaces and whether each explained unique variance in the multidimensional trait space. Both routes were associated with and uniquely contributed to trait impressions in both samples. At the individual-trait level, associations were more selective in the U.S. sample but broader in the Chinese sample: visual representations were especially associated with femininity and physical strength, whereas semantic representations also tracked criticalness and practicalness. Familiarity with the target further moderated route-specific associations, amplifying semantic alignment for practicalness and competence in the Chinese sample. In the U.S. sample, recognition increased semantic alignment for physical strength and reduced visual alignment for practicalness. These findings show that facial trait impressions reflect both visual appearance and public semantic information, with route-specific contributions varying across traits and contexts.

Keywords: facial trait impressions; person perception; conceptual knowledge; familiarity; representational similarity analysis; social cognition

Introduction

Forming facial trait impressions is a ubiquitous and influential aspect of human social cognition. Within milliseconds of encountering a face, a perceiver can form a rapid and automatic impressions about a target's social traits, such as trustworthiness and dominance (Oosterhof & Todorov, 2008; Todorov et al., 2015; Willis & Todorov, 2006), even when the perceiver is instructed not to make such judgments (Ritchie et al., 2017). These trait inferences from faces, regardless of accuracy, can have far-reaching consequences in various domains of social life, from hiring decisions (Olivola et al., 2014), political elections (Todorov et al., 2005) and criminal sentencing (Wilson & Rule, 2015; Zebrowitz & McDonald, 1991). For example, job candidates with faces perceived as more competent are more likely to receive job offers (Olivola et al., 2014); similarly, political candidates with competent looking faces are more likely to win elections, regardless of their actual qualifications or performance (Todorov et al., 2005). Facial impressions may also affect criminal justice outcomes: untrustworthy-looking defendants receive harsher sentences (Wilson & Rule, 2015), while baby-faced ones are more likely to win intentional-harm cases but lose negligence claims (Zebrowitz & McDonald, 1991).

Social Trait Space

How are the many social traits that a face can convey mentally organized? Influential theories posit that facial impressions are structured by a small number of broad evaluative dimensions, such as trustworthiness and dominance (Abele et al., 2016; Fiske et al., 2007; Judd et al., 2005; Oosterhof & Todorov, 2008), or warmth/communion and competence/agency (Abele & Wojciszke, 2014; Fiske et al., 2007). The rationale for these two-dimensional accounts

is that these evaluative dimensions capture information highly relevant for social interaction: one concerns others' intentions toward us, and the other concerns their capacity to act on those intentions. In recent years, however, research suggests that trait impression space may be richer than two dimensions, with additional dimensions emerging when a broader range of traits, perceivers or more naturalistic stimuli were included (Connor et al., 2024; Freeman & Lin, 2025; Koch et al., 2016; Lu & Lin, 2025; Nicolas et al., 2022; Vernon et al., 2014). More importantly, research argues that face trait space may reflect a dynamic integration of not only intrinsic facial-feature covariation but also conceptual associations, stereotypes, and other social cognitive factors (Illithova et al., 2025; Stolier et al., 2018; Zhao et al., 2024). These models highlight the potential richness and multidimensionality of person perception while raising important questions about what sources of information contribute to them.

To explain how impressions are formed, a substantial body of literature has examined how individuals extract trait-relevant information from facial appearance, converting perceptual features to social trait impressions (Oosterhof & Todorov, 2008; Sutherland et al., 2013; Todorov et al., 2015). For example, facial width-to-height ratio shaped dominance and aggression judgments toward men (Geniole et al., 2014; Mileva et al., 2014). Face shape and reflectance differentially predicted traits such as dominance and competence (Oh et al., 2019). Furthermore, valence judgements linked to resemblance to emotional expressions and dominance judgement linked to cues of physical strength (Oosterhof & Todorov, 2008; Said et al., 2009; Todorov, 2008; Toscano et al., 2014). Together, these findings show that facial appearance provides a rich perceptual basis for trait impressions, with different visual cues supporting different social inferences.

Conceptual Contributions to Trait Impression

Yet social trait impressions rarely arise from the appearance of faces alone. Faces are often accompanied by conceptual information, including names, occupations, group memberships, reputations and other forms of knowledge that may also structure trait impressions (Freeman & Chwe, 2024; Oh et al., 2021). Such conceptual knowledge can influence impressions at multiple levels. At the category level, stereotypes, as forms of conceptual knowledge tied to social categories, shape trait impressions, including gender (Oh et al., 2020), race (Xie et al., 2021), and inferences about occupation and status (Imhoff et al., 2013; Oldmeadow et al., 2013). At the target level, learned information can override the effect of appearance (Amodio, 2025; Chua & Freeman, 2021; Lin & Thornton, 2024; Shen et al., 2020). For example, learning positive information about targets with untrustworthy-looking faces can shift trait judgments in a positive direction, and vice versa (Cone et al., 2017; Shen et al., 2020). Such conceptual effects can spread to other perceptually similar targets: affective learning about a face generalizes to perceptually similar faces (Verosky & Todorov, 2010), incidental resemblance to known individuals biases automatic evaluation (Gawronski & Quinn, 2013), and stimulus generalization based on appearance supports learning whom to trust (FeldmanHall et al., 2018). Finally, conceptual knowledge can vary idiosyncratically across perceivers. For example, perceivers' beliefs about how traits covary shape how similarly they judge faces across those traits, such that an individual's conceptual trait structure predicts the structure of their facial impressions (Stolier et al., 2018; Xie et al., 2021). These idiosyncratic structures may also reflect perceivers' own personalities, social environments, cultural beliefs, or accumulated social experiences (Cook et al., 2022; Oh et al., 2022; Stolier et al., 2020; Sutherland et al., 2020). Despite growing recognition of conceptual contributions to face-based impressions, we still

know relatively little about how visual appearance and conceptual knowledge jointly contribute to trait impressions: how much they reflect the facial appearance itself, how much they reflect the knowledge of the person, and whether each source explains unique variance. Addressing this gap requires treating facial appearance and conceptual knowledge as comparable representational spaces measured in the same targets and related to the same trait impression.

The insight that social trait impressions are formed on the basis of both conceptual and perceptual information is formalized in the Dynamic Interactive Model of person perception (Freeman et al., 2020; Freeman & Ambady, 2011). This model posits that top-down conceptual information and bottom-up perceptual input interact continuously to yield social perception rather than operating as separate stages. Empirical work supports the framework that conceptual information about group membership interactively shaped face processing (Brooks & Freeman, 2018). The model reframes impressions as the joint product of perception and knowledge and provides a synthetic framework that organizes empirical findings in social trait impression. However, this framework has focused on category-level knowledge (e.g., group-based prejudice), experimentally learned information about unfamiliar targets or perceiver-specific belief structures. Less is known about how naturally acquired person-specific knowledge about real individuals contributes to trait impressions.

A Dual-route Model of Face-based Social Trait Impression

Here, we propose and provide evidence for a dual-route model of social trait impressions from faces (**Figure 1**). The model posits that face-based social trait impression relies on two

distinct but interacting routes. A perceptual route maps observable cues onto trait impressions[1], and a conceptual route maps the perceiver's knowledge about the person, such as group memberships, personal experiences, and biographical information, onto the same trait impressions.

Testing this framework requires quantifying the perceptual and conceptual routes in comparable terms, which is made possible by recent advances in computational modeling. Computer vision models trained to recognize faces provide a quantitative model of the perceptual information in a face image (Q. Cao et al., 2018; Dobs et al., 2023), and research has shown that such models can predict human trait judgments (Parde et al., 2019; Peterson et al., 2022). Large language models can recover human knowledge and predict social trait perception and similarity judgments (X. Cao & Kosinski, 2024; Charest et al., 2014; Chen et al., 2024; Grand et al., 2022).

However, even though these models can capture the perceptual and conceptual information of a face image respectively, these models are incommensurable with social traits and with one another. One way of integrating information with different dimensions is through representational geometry. For a set of face images, one can construct their representational geometry by calculating pairwise dissimilarity of those face images in terms of social traits, and model-based visual and conceptual information, typically referred to as representational dissimilarity matrices (RDMs) (Kriegeskorte, 2008). In the language of RDM, the dual-route model can be described as – the representational geometry of social trait impression can be

[1]Although perceptual cues may include the facial appearance, voice (Irvine & Lavan, 2026; Lavan et al., 2024), and body (Hu et al., 2018), the present study focuses specifically on facial appearance as the visual component of this route.

explained uniquely and jointly by the representational geometry of the perceptual information of the faces and the conceptual information of the identities.

The Present Research

We apply this approach to facial trait impressions of celebrities. Celebrities offer an opportunity to study the impression of faces that carry person-specific conceptual knowledge, as such information is publicly available and has good public exposure. We recruited two samples of participants from the U.S. and China to rate celebrity faces on several social traits, such as warmth and competence. We constructed the visual and semantic representational geometry based on computer vision model analysis of face images and large language model analysis of the celebrities' publicly available textual description.

We test three hypotheses. First, both the perceptual and conceptual routes will be associated with the representational geometry of facial trait impressions (H1). Second, each route will explain unique variance in trait impressions (H2).

Third, we examined whether perceivers' familiarity with target celebrities shifts the relative weighting of the two routes. Classic accounts of impression formation describe a shift from category-based to person-specific processes as perceivers become familiar with a target (Brewer, 1988; Fiske & Neuberg, 1990). Impressions of unfamiliar others are therefore expected to rely more on perceptual cues, social categories and stereotypes, whereas impressions of well-known targets can draw on prior interactions, accumulated knowledge or target-specific associations (Kunda & Thagard, 1996). Consistent with this account, familiar faces are not processed simply as more recognizable visual stimuli (Kramer et al., 2018); their processing involves retrieving the identity behind the face (Burton et al., 2016), along with the prior

experience, person knowledge and affective evaluations (FeldmanHall et al., 2018; Gobbini & Haxby, 2007; Ramon & Gobbini, 2018; Thornton & Mitchell, 2017; Todorov et al., 2007; Young & Burton, 2018). At the same time, familiarity supports invariant recognition across changes in appearance (Burton et al., 2016; Kramer et al., 2018; Young & Burton, 2018), potentially reducing reliance on currently visible facial cues. We therefore hypothesize that familiarity will modulate the contributions of the perceptual and conceptual routes, with greater familiarity increasing semantic contribution to facial trait impressions (H3).

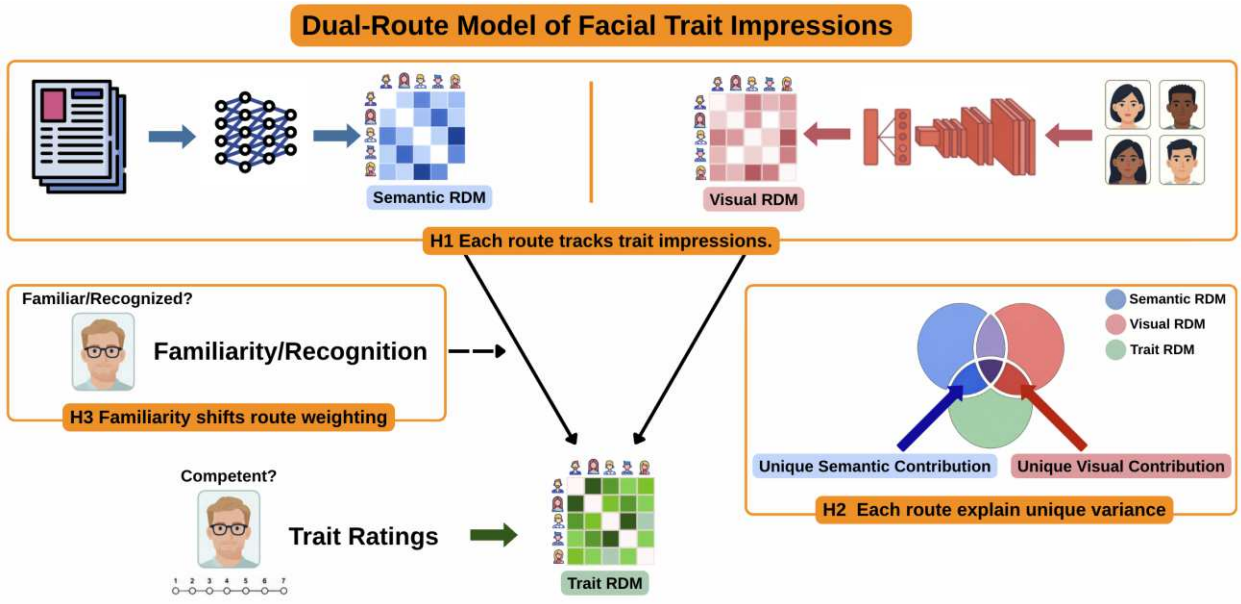


Figure 1. The Dual-Route Model of Facial Trait Impressions. A schematic illustrating how a facial trait impression derives from two sources of information. The conceptual route derives semantic representations from encyclopedic descriptions of each target using a large language model, yielding a semantic RDM. The perceptual route derives visual representations from face images using a vision model, yielding a visual RDM. Both model RDMs are compared with the behavioral trait RDM constructed from participants' trait ratings. H1 tests whether each route tracks the structure of trait impressions using representational similarity analysis; H2 tests

whether the two routes explain unique variance in the behavioral trait RDM using variance partitioning; and H3 tests whether familiarity or recognition shifts the relative weighting of the semantic and visual routes using moderation analysis in linear mixed models.

Methods and Materials

Participants

For Experiment 1, we recruited a U.S. convenience sample ($N = 415$) via Prolific (mean age = 26.35 years, $SD = 7.14$; 156 female; 279 White/Caucasian, 76 Latino/Hispanic, 18 Middle Eastern, 15 Mixed, 6 East Asian and 21 other race/ethnicity). Part of this sample was reported in a previously published study (Yu et al., 2022). Experiment 1 was approved by the Institutional Review Board of West Virginia University (IRB reference number: 1709745061).

For Experiment 2, we recruited 330 Chinese college students from Shenzhen University. Three participants were excluded based on the pre-registered criteria detailed in the *Procedure* section, yielding a final analytic sample of 327 participants (mean age = 25.26 years, $SD = 7.51$; 188 female). Sample size was determined a priori based on prior work showing that stable average trait ratings can be obtained with 22–29 raters per stimulus based on our selected traits (Hehman et al., 2018; Lin et al., 2021). Therefore, we aimed for 30 independent raters per face per trait, yielding a target sample of 300 raters and oversampled by 10% to account for exclusions, resulting in a recruitment target of 330 participants. The design, exclusion criteria, and primary analyses for Experiment 2 were preregistered (AsPredicted #239035). Experiment 2 was approved by the Institutional Review Board of Shenzhen University (IRB reference number: SZU_PSY_2024_150).

Materials

Visual stimulus construction

For Experiment 1, we selected 50 celebrities from the CelebA dataset (Liu et al., 2015) and obtained 10 distinct naturalistic photos for each, yielding a total of 500 face images. The selected identities represented a range of genders and racial backgrounds: 33 were male, 40 were White, 9 were Black, and 1 was biracial. The images varied in facial angle, gaze direction, background, lighting, expression, and the presence of accessories (e.g., glasses, hats).

For Experiment 2, we curated a stimulus set for Asian celebrities similar to the CelebA dataset, which we name UCSB-SZU-Celeb, to complement the Western celebrity stimuli used in Experiment 1. We intentionally included better known celebrities in this stimulus set, so that our familiarity could have a more balanced trial structure. The stimulus selection procedure involves two major steps: first, target identity selection, and second, face image collection and standardization.

Target identity selection and evaluation. Seven Chinese psychology researchers nominated well-known Chinese celebrities. Each nominator was instructed to provide 10–15 names of Asian celebrities with whom they were familiar, spanning a broad range of occupations, including entertainment, sports, politics, business, and researchers and writers. After removing duplicates, an initial pool of 75 celebrities (38 male, 37 female) was compiled. A separate group of seven Chinese undergraduate research assistants (5 female; mean age = 22 years, *SD* = 1.58) then rated their familiarity with each target on a 5-point scale. Fifty celebrities (25 female) were selected as stimuli for Experiment 2 based on the following criteria: (a) the average familiarity rating exceeded 4; (b) all individual familiarity ratings were greater than 1 (not recognized at all); (c) male celebrities at the lower end of the familiarity range were

excluded to ensure gender balance and occupation diversity; and (d) celebrities from substantially older generations, such as Chen-Ning Yang, were excluded. Descriptive statistics are reported in *Supplementary Materials*.

Face image collection and standardization. For the 50 selected celebrities, 15–20 recent, high-quality images per target identity were initially collected from publicly accessible online sources (e.g., Baidu, Weibo). Inclusion criteria required that faces be clearly visible, front-facing, and of high resolution. The selected images were then standardized through the following steps: images were cropped to remove regions below the shoulders, retaining only the core facial area (passport-style framing), and resized to a uniform resolution of 172 × 218 pixels as the CelebA images. Following quality control, 10 representative images were retained for each target, yielding a final set of 500 standardized face stimuli. These images were used to construct the visual representational space for each target. Example stimuli are shown in **Figure 2**.

Textual corpus construction

In addition to the face images used to construct the visual representational space, we collected textual descriptions of each target to operationalize the conceptual route. For each U.S. target, we scraped their corresponding Wikipedia article. Similarly, for each Chinese target, the corresponding Baidu Baike (a Chinese equivalent of Wikipedia) entry was collected as the primary textual corpus for semantic embedding (see below). As the article lengths vary across celebrities, we selected the first substantive paragraph for further analysis, which includes the key information such as demographic information, professional achievements, career history, and public evaluations (U.S.: M = 185.6 words, SD = 137.8; Chinese: M = 318.6 characters, SD = 173.5).

Procedure

Face Judgment Task. Participants completed an online rating task in which they evaluated each target' face images on 8 social traits using a 7-point Likert scale. The traits included warmth, criticalness, competence, practicality, femininity, strength, youthfulness, charisma, trustworthiness, and attractiveness. These trait dimensions have been established and used to provide a comprehensive trait space in prior studies (R. Cao et al., 2023; Lin et al., 2021; Yu et al., 2022). In the Chinese sample, participants rated celebrities on 10 traits, comprising the eight traits shared with the U.S. sample and two additional traits: trustworthiness and attractiveness. In each trait block, the corresponding trait word with its definition was presented before rating trials; on each trial, a face image was presented together with one trait word, and participants indicated the extent to which the trait described the target person using a 7-point Likert scale. Higher ratings indicated stronger perceived endorsement of the trait. The participants also reported their familiarity with each target: the U.S. participants rated whether they recognized the target (0 = do not recognize, 1 = recognize) and the Chinese participants rated their familiarity with the target on a scale of 1-7 (1= do not recognize, 7 = very familiar).

Both experiments followed the same procedure. The full stimulus set consisted of 500 face images (50 targets × 10 images per target), which were randomly distributed into 10 modules, with each module containing one unique image per target. Each participant was randomly assigned to one module and rated all faces on each of the traits, presented in separate trait blocks. The order of trait blocks was counterbalanced across modules, and modules were randomly assigned to participants. This design ensured that each image of each target was evaluated across traits while minimizing within-subject fatigue and controlling for order effects.

Data were screened prior to analysis using three criteria. First, at the trial level, responses with reaction times shorter than 100 ms or longer than 5,000 ms were excluded. Second, at the block level, an entire trait block was removed for a given participant if more than 30% of its trials were excluded based on the reaction time criterion, or if the participant used fewer than three distinct response values within that block, indicating insufficient use of the rating scale. Third, at the participant level, individuals were excluded if more than three blocks were removed according to the block-level criteria. On average, these procedures resulted in the exclusion of fewer than 5% of trials per participant. In the U.S. sample, on average, each image module was assigned to 41 participants; after exclusion, an average of 39 valid ratings were retained for each image on each trait. In the Chinese sample, 33 participants were assigned to each module; after exclusion, an average of 32 valid ratings were retained for each image on each trait.

For the U.S. participants (Experiment 1), the instructions and questions were presented in English, while for the Chinese participants (Experiment 2), the instructions and questions were presented in Chinese, which followed a standard translation/back-translation procedure by Chinese-English bilingual researchers.

Participants also reported demographic information, including age, sex, highest level of education, and subjective socioeconomic status (SES).

Analysis

Visual representational space. The perceptual route was operationalized as a visual representational space derived from a deep face-recognition network based on each target's images in the stimuli set. Each face image was passed through an InceptionResNet-V1 FaceNet model pretrained on VGGFace2, a convolutional neural network trained for face identification

(Q. Cao et al., 2018), which generated its feature vector. This model provides a compact 512-dimensional embedding optimized for facial identity discrimination. VGGFace2 contains large natural variation in pose, age, illumination, and identity, making it appropriate for estimating identity-relevant visual similarity among face images (Dobs et al., 2023; Lee et al., 2026; Parde et al., 2019; Ramesh et al., 2022; Tea-makorn & Kosinski, 2020). The 512-dimensional embeddings were extracted from activations of the penultimate layer because it is the model's face-descriptor output before identity classification, preserving high-level facial identity information while avoiding dependence on the specific training identities. Then we averaged the visual embeddings across images as a single visual feature vector for each target.

Semantic representational space. The conceptual route was operationalized as a semantic representational space derived from text embeddings of each target's encyclopedic description. This semantic space was intended to capture publicly available person knowledge encoded in biographical text. Importantly, we do not assume that participants explicitly retrieved these encyclopedic descriptions when making trait judgments. Rather, we test whether the structure of facial trait impressions tracks publicly available semantic representations of the same identities. Specifically, we collected a Wikipedia-style biographical description and segmented the text into individual sentences. Each sentence was submitted separately to the OpenAI embedding model to obtain a 3,072-dimensional semantic vector. Sentence-level embedding was used to preserve local semantic information. For each target, sentence embeddings were then averaged across all available sentences to a single target-level vector.

Trait representational spaces. The outcome space was operationalized as a behavioral trait representational space derived from perceivers' ratings of each target. Specifically, we constructed an omnibus social-trait space capturing the trait profiles of celebrities across the full

set of rated traits. For each target, we created a multi-dimensional vector consisting of its mean trait ratings on eight traits: warmth, criticalness, competence, practicality, femininity, strength, youthfulness, and charisma. This omnibus space provided a summary measure of how each target was perceived across the broader social-trait profile.

In addition to the overall trait representational space, we also constructed trait-specific representational spaces capturing how differently each pair of celebrities was perceived on that trait. Specifically, for each target, ratings were averaged across valid perceivers to obtain a single trait score. This procedure yielded one trait representational space for each dimension. These trait-specific spaces allowed us to test whether the visual and semantic routes contributed differently across distinct kinds of social impressions, complementing the multi-dimensional trait-space analyses.

Representational Similarity Analysis (RSA). Representational Similarity Analysis provides a framework for comparing the structure of representations across different modalities by evaluating whether they organize the same set of stimuli in similar ways (Kriegeskorte, 2008; Popal et al., 2019). Specifically, each domain is first converted into a representational dissimilarity matrix (RDM), in which each cell reflects the pairwise dissimilarity between two target identities. In this study, the visual RDM captured how dissimilar two celebrities were in face-model embedding space, the semantic RDM captured how dissimilar they were in text-embedding space, and the trait RDM captured how differently they were judged on social traits. RSA then tested whether celebrities who were visually or semantically similar were also perceived as similar in each trait space. This allowed us to assess whether facial trait impressions were associated with visual facial information and semantic person knowledge on a common representational scale.

Trait RDMs. For the multidimensional trait space, we constructed one 50 × 50 RDM per dataset by computing pairwise Euclidean distances between target identities across the eight trait dimensions shared by the U.S. and Chinese samples: warmth, criticalness, competence, practicality, femininity, strength, youthfulness, and charisma. To ensure comparability across datasets, the two additional traits collected only in the Chinese sample, i.e., attractiveness and trustworthiness, were excluded from the multidimensional trait-space analysis. Because this analysis produced a single trait-space outcome per dataset, no correction for multiple comparisons was applied.

For the trait-specific analyses, we constructed separate 50 × 50 RDMs for each individual trait. These analyses included all traits available within each dataset. Because these models tested multiple trait-specific outcomes, statistical significance was corrected across traits using the maximal permutation procedure described below.

Semantic and Visual RDMs. To model the representational geometry of the stimulus set, we constructed two model-based RDMs capturing semantic and visual similarity between target identities. Semantic and visual RDMs were computed as pairwise cosine distances between visual and text embeddings of targets, respectively.

For each trait space, we computed Spearman correlations between the trait RDM and each model-based RDM (visual and semantic), allowing us to quantify how closely human trait impression encodes each information source. To assess statistical significance of each route, we used nonparametric permutation testing: we randomly permuted the target labels of the trait RDM and recalculated the RSA correlation for 5,000 iterations, which formed a null distribution. The *p*-value was derived by comparing the observed correlation to this null distribution. This procedure was conducted separately for the perceptual and conceptual route. For each trait, we

compared the magnitudes of the two routes by testing the difference between the two correlations with bootstrapping. Specifically, on each of 5,000 resamples of the 50 targets drawn with replacement we rebuilt all three RDMs, dropped the pairs in which a duplicated target met itself, and recomputed the difference $\rho_{semantic} - \rho_{visual}$. We reported the percentile 95% confidence interval and a two-sided p_{boot} from the proportion of resamples falling on either side of zero.

Variance partitioning. To quantify the unique contributions of perceptual and conceptual information to trait impressions, we implemented variance partitioning analysis (Groen et al., 2018; Lin & Thornton, 2024; Ray-Mukherjee et al., 2014). This method allowed us to decompose the variance in trait RDMs into components uniquely explained by each source of information, i.e., visual and semantic RDMs. Specifically, for each trait, we performed multiple linear regression in which the trait RDM served as the dependent variable, and the visual and semantic RDMs were entered as predictors. This full model yielded a total proportion of variance in the trait RDM that can be explained by the two predictor RDMs jointly. To isolate the unique contribution of each predictor RDM, we then estimated two partial models, where we dropped one of the two predictors. The variance uniquely explained by the semantic RDM was computed as the difference in explained variance (i.e., R^2) between the full model and the visual-only model. Similarly, the variance uniquely explained by the visual RDM was computed as the difference in explained variance between the full model and the semantic-only model.

The significance of each unique contribution was determined by nonparametric permutation testing. Specifically, we shuffled the target labels of the trait RDM and recomputed the unique variance for 5,000 iterations to build a null distribution. Bootstrapping over targets was used separately to obtain confidence intervals and to compare the semantic and visual unique variance. We resampled the 50 targets with replacement 5,000 times, discarded the pairs

in which a duplicated target met itself, recomputed the unique variance, and took the 2.5th and 97.5th percentiles as a 95% confidence interval. This yielded the difference in unique variance with its percentile interval and a two-sided p_{boot}.

The trait space is a single outcome by construction and therefore does not need multiple comparisons correction. The per-trait permutation p values were corrected with a max-T procedure over the same permutations to control for the family-wise error rate within each channel and each dataset.

Familiarity Moderation

For the familiarity analysis, we fit linear mixed-effects models to representational distances computed across all pairs of targets viewed by a given participant. For each trait, the dependent variable was the Euclidean distance between a participant's ratings of two targets. Semantic and visual distances were properties of the target pair and were therefore identical across participants, whereas familiarity varied across participant-target trials. The absolute familiarity difference between the two targets was included as a control. All predictors were z-scored before model fitting.

The model tested whether the mean familiarity of the two targets moderated the association of semantic and visual distances to trait representations:

$$\begin{aligned}\textit{Trait Distance} \sim\ & \textit{(Semantic Distance + Visual Distance)} \times \textit{Familiarity Mean} + \\ & \textit{Familiarity Difference} + \\ & \textit{(1 + (Semantic Distance + Visual Distance)} \times \textit{Familiarity Mean} \mid \textit{Participant)} + \\ & \textit{(1 + (Semantic Distance + Visual Distance)} \times \textit{Familiarity Mean} \mid \textit{Target}_{A}\textit{)} +\end{aligned}$$

$$(1 + (\text{Semantic Distance} + \text{Visual Distance}) \times \text{Familiarity Mean} \mid \text{Target}_B)$$

Mean familiarity was defined as the average familiarity score of the two targets in a pair, which allowed us to examine if overall familiarity with the targets amplifies the contribution of the semantic and/or visual information to trait representations. Specifically, a positive interaction effect would mean that semantic and/or visual information plays a greater role in explaining social impressions of better-known targets. To account for repeated observations and stimulus-specific dependencies, we included random intercepts and random slopes of all effects of interest for participants, and each target of the pair. Because the two samples measured familiarity differently, we describe the Chinese moderator as familiarity (a graded seven-point item) and the U.S. moderator as recognition (a binary judgement); we return to this asymmetry below. Models were fitted by maximum likelihood in glmmTMB (Brooks et al., 2017) over 373,388–389,137 participant × target-pair observations from 321–326 Chinese participants and 433,689–489,741 observations from 384–415 U.S. participants. Statistical significance was reported at $p < .05$ (uncorrected), unless otherwise noted. We also applied Holm–Bonferroni correction within each dataset and channel for trait specific models to control for the family-wise error rate.

Random-effects specification. We initially specified a maximal random-effects structure to account for repeated observations within participants and dependencies introduced by the repeated use of target identities across dyads. This approach follows recommendations to include random intercepts and random slopes for analytically relevant effects when estimating fixed effects in repeated-measures and crossed-stimulus designs (Barr et al., 2013; Judd et al., 2012), as well as prior applications in person-perception research (Kramer & Jones, 2020). The initial model included random intercepts and random slopes for the effects of interest by each participant and by each target in the pair (L0). We then evaluated the random-effects structure

using likelihood-ratio tests, model convergence, Hessian diagnostics, and estimated random-effect variances. When the maximal model failed to converge or contained unsupported variance components, the random slopes were reduced progressively while holding the fixed-effects structure constant (Matuschek et al., 2017). Reduction followed the higher-order-to-lower-order sequence, as shown in **Table 1**: target-specific random slopes for interaction effects (L1), target-specific random slopes for familiarity main effects (L2), target-specific random slopes for semantic and visual main effects (L3), and finally participant-level random slopes in the same order (L4-L6). This procedure allowed the models to account for meaningful heterogeneity across participants and targets while avoiding overparameterized random-effects structures that were not supported by the data.

The maximal structure was selected for 15 of the 20 outcomes. Reduction was required for five: criticalness in the Chinese sample (L2); practicalness in the Chinese sample (L1); warmth in the Chinese sample (L1); competence in the U.S. sample (L1); criticalness in the U.S. sample (L1). In every one of these the model retained is at L1 or L2, so the perceiver-level slopes for both focal interactions are present in all 20 models reported in the main text.

Table 1.

Levels of the pre-specified reduction ladder.

Level	Perceiver	Target 1 and Target 2 (each)	*k*
L0	1 + S + V + F + S×F + V×F	1 + S + V + F + S×F + V×F	63
L1	1 + S + V + F + S×F + V×F	1 + S + V + F	41

L2	1 + S + V + F + S×F + V×F	1 + S + V	33
L3	1 + S + V + F + S×F + V×F	1	23
L4	1 + S + V + F	1	12
L5	1 + S + V	1	8
L6	1	1	3

Note. S = semantic distance, V = visual distance, *F* = pair-mean familiarity. *k* = number of covariance parameters.

Throughout the paper, we use "perceptual route" and "conceptual route" to refer to the theoretical sources of facial trait impressions. In the present analyses, the perceptual route was operationalized as a visual representational space derived from face-recognition model embeddings, whereas the conceptual route was operationalized as a semantic representational space derived from text embeddings of public encyclopedic descriptions. We therefore use "visual model" and "semantic model" when referring to the measured RDMs, and reserve "perceptual" and "conceptual" for the broader theoretical framework.

Results

Inter-rater consistency across facial trait impressions

We first assessed the extent to which participants showed shared impressions of the target faces across the social traits. To estimate group-level consistency, we decomposed the variance in individual-level ratings using null multilevel models with random intercepts for target, participant, and image set module (Hehman et al., 2017). The resulting intraclass correlation coefficients (ICCs) quantify each source's share of total rating variance. At the level of the multidimensional trait space, target accounted for a share of rating variance in both datasets (U.S.: ICC_{target} = .048; China: ICC_{target} = .043), comparable to the participant-level share (U.S.: $ICC_{participant}$ = .035; China: $ICC_{participant}$ = .033) and far exceeding the image-module-level share (both ICC_{image} < .001). The image set module was therefore treated as a negligible source of variance requiring no explicit control in our analysis. Because these values quantify the proportion of total multidimensional rating variance attributable to each source and trait-level mean differences also contribute to the residual variance, conventional inter-rater reliability thresholds do not apply here. We report these variance components primarily to establish that the image-set module contributed negligible variance to the ratings.

When it comes to specific traits, the proportion of rating variance attributable to target ranged from .064 to .772 across traits in the U.S. sample (M = .243) and from .099 to .851 in the Chinese sample (M = .293). Target reliability was highest for the most physically grounded traits, femininity (U.S. ICC_{target}= .772; China ICC_{target} = .851) and youthfulness (U.S. ICC_{target} = .476; China ICC_{target} = .644). In both datasets, the variance attributable to the image modules was negligible across all traits (U.S. ICC_{image} range: .000–.003, M = .000; China ICC_{image} range: .000–.002, M = .001), far below the participant-level component (U.S. $ICC_{participant}$ range: .031–.153, M = .102; China $ICC_{participant}$ range: .010–.155, M = .109). These reliabilities

indicate that target-level impressions were consistent enough across raters to support the following analyses. Detailed statistics are reported in *Supplementary Materials*.

To further evaluate the validity of these ratings, we sorted the faces along each trait dimension by ranking identities from low to high mean scores and visualized the top five and bottom five identities (**Figure 2**). These visual continua revealed clear and interpretable trait gradients. For youthfulness, the ordered faces showed a visible transition from older-appearing to younger-appearing identities. For femininity, the sequence progressed from more typically masculine to more typically feminine facial appearance. For competence, higher-rated faces tended to convey a more mature, composed, and agentic social impression. Together, these results suggest that participants' ratings captured meaningful variation in perceived social traits across targets.


US Trait Rating Extremes
Lowest-rated targets
Highest-rated targets
Warm
Critical
Competent
Practical
Feminine
Strong
Youthful
Charismatic
Lowest
Highest

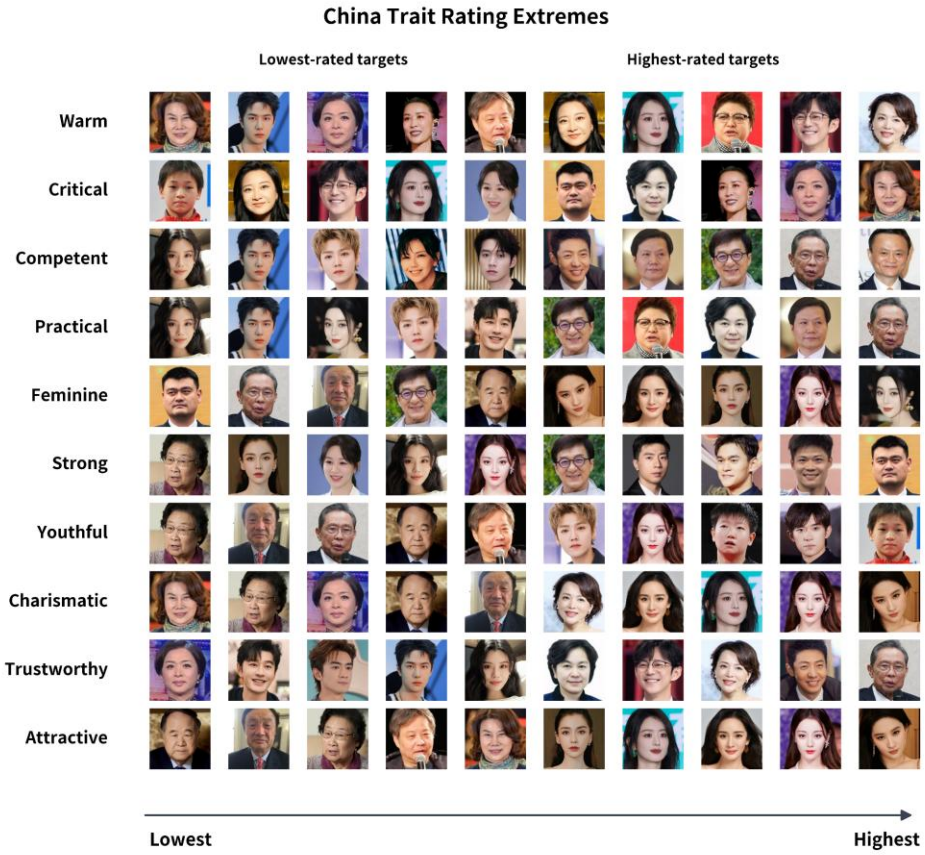

China Trait Rating Extremes
Lowest-rated targets
Highest-rated targets
Warm
Critical
Competent
Practical
Feminine
Strong
Youthful
Charismatic
Trustworthy
Attractive
Lowest
Highest

Figure 2. Example photos with high and low average trait ratings (upper panel: U.S. sample; lower panel: Chinese sample).

Associations between social trait representation and visual and semantic structures

We next examined whether social trait representations at the trial level could be explained by two sources of information: visual features of the faces and semantic information about the identities. To illustrate the distribution of the target identities in the high-dimensional visual and semantic spaces, we reduced the visual and semantic high-dimensional spaces to 2-dimension spaces using t-distributed Stochastic Neighbor Embedding (t-SNE). In the figure depicting the visual space (**Figure 3**), identities that are physically similar to each other (e.g., appearance of gender, skin tone, etc.) are closer, whereas in the semantic space, identities who have similar occupations are closer to each other (**Figure 4**).

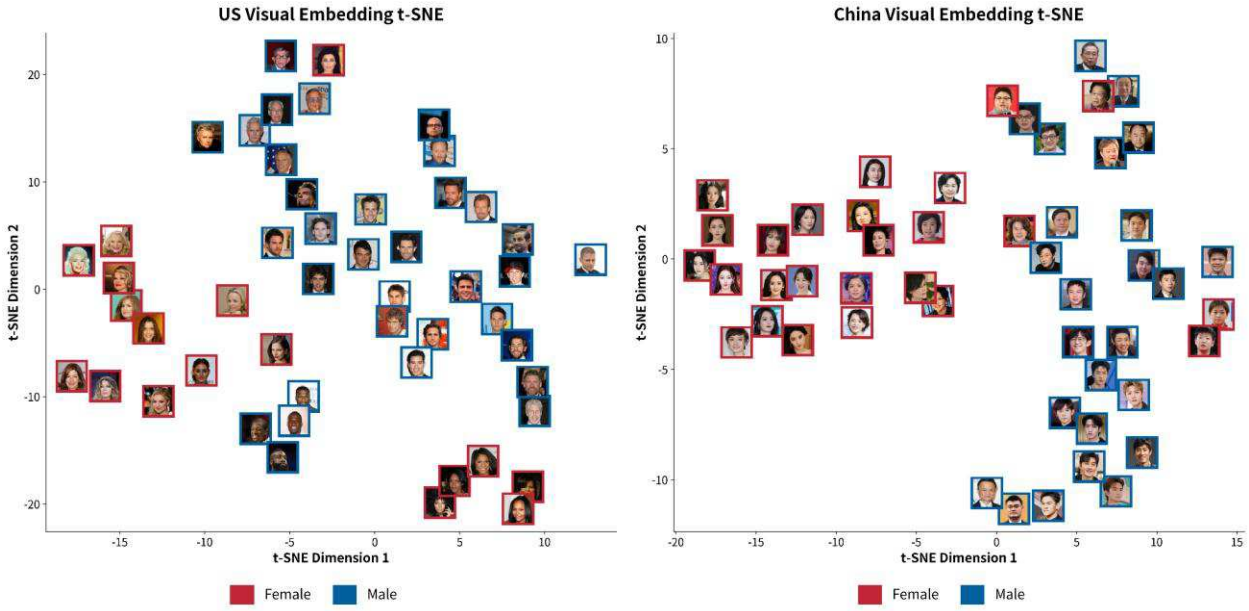


Figure 3. t-SNE projections of the target identities in the visual embedding space. Left: U.S. sample; right: Chinese sample. Thumbnail borders are color-coded by gender.

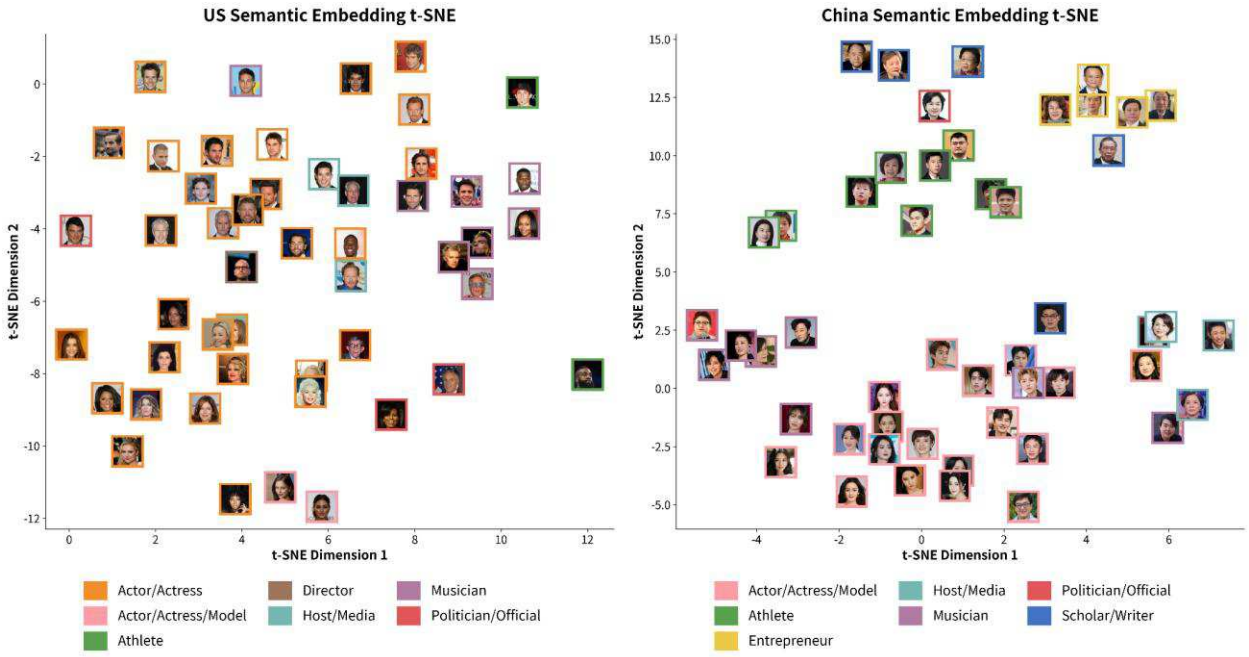


Figure 4. t-SNE projections of the target identities in the semantic embedding space. Left: U.S. sample; right: Chinese sample. Thumbnail borders are color-coded by occupation category.

Both routes are associated with trait-impression structure (H1)

Next, we tested whether the visual and semantic spaces were associated with the representational structure of trait impressions.

Trait-space RSA showed that both semantic and visual representational spaces were significantly associated with the behavioral trait space in both datasets (**Figure 5**). In the U.S. sample, the semantic space was positively associated with the trait space across all targets ($\rho = .36$, $p_{perm} < .001$), as was the visual space ($\rho = .32$, $p_{perm} < .001$). The two associations did not differ significantly ($\Delta\rho = .04$ [−.18, .27], $p_{boot} = .679$). In the Chinese sample, both

representational spaces were also significantly associated with the trait space (semantic: ρ = .39, p_{perm} < .001; visual: ρ = .69, p_{perm} < .001). Moreover, the semantic association was substantially weaker than the visual association (Δρ = −.30 [−.45, −.13], p_{boot} < .001). Thus, trait-space RSA indicated that both semantic and visual models tracked the organization of trait impressions, with comparable strength in the U.S. sample but a stronger visual association in the Chinese sample.

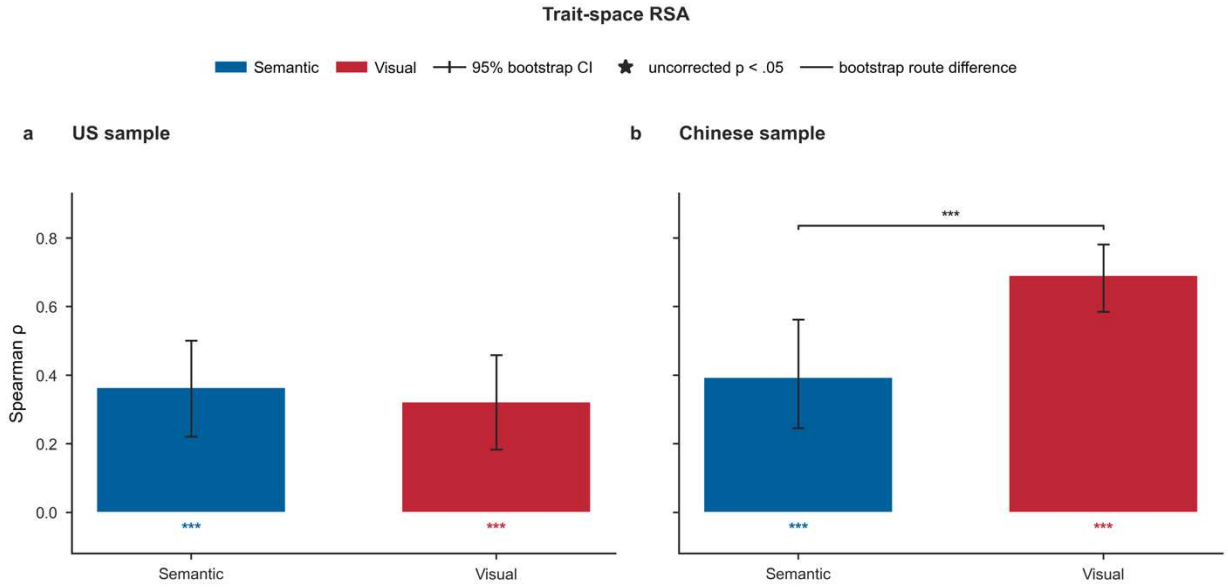


Figure 5. Correlations between the multidimensional social-trait space and the visual and semantic spaces in the (a) U.S. sample and (b) Chinese sample. Colored asterisks indicate the significance of the association between the multidimensional trait RDM and each model RDM based on permutation tests: semantic RDM (blue) and visual RDM (red). Black asterisks indicate a significant level of difference between the semantic and visual associations, based on paired bootstrap resampling of the 50 targets. *: < .05, **: < .01, ***: < .001.

We next examined individual social traits separately. For the U.S. data, the semantic model correlated significantly with the impression structure of femininity (ρ = .34, p_{perm} < .001) and physical strength (ρ = .18, p_{perm} = .007), as shown in **Figure 6**. The visual model correlated significantly with the same two traits, femininity (ρ = .24, p_{perm} < .001) and physical strength (ρ

= .19, $p_{perm} < .001$) and additionally with youthfulness ($\rho = .16$, $p_{perm} < .001$) and practicalness ($\rho = .09$, $p_{perm} = .017$). Comparing the two routes at the identity level, however, no U.S. trait showed a significant difference between them. The two routes did not differ on trait impressions in this sample.

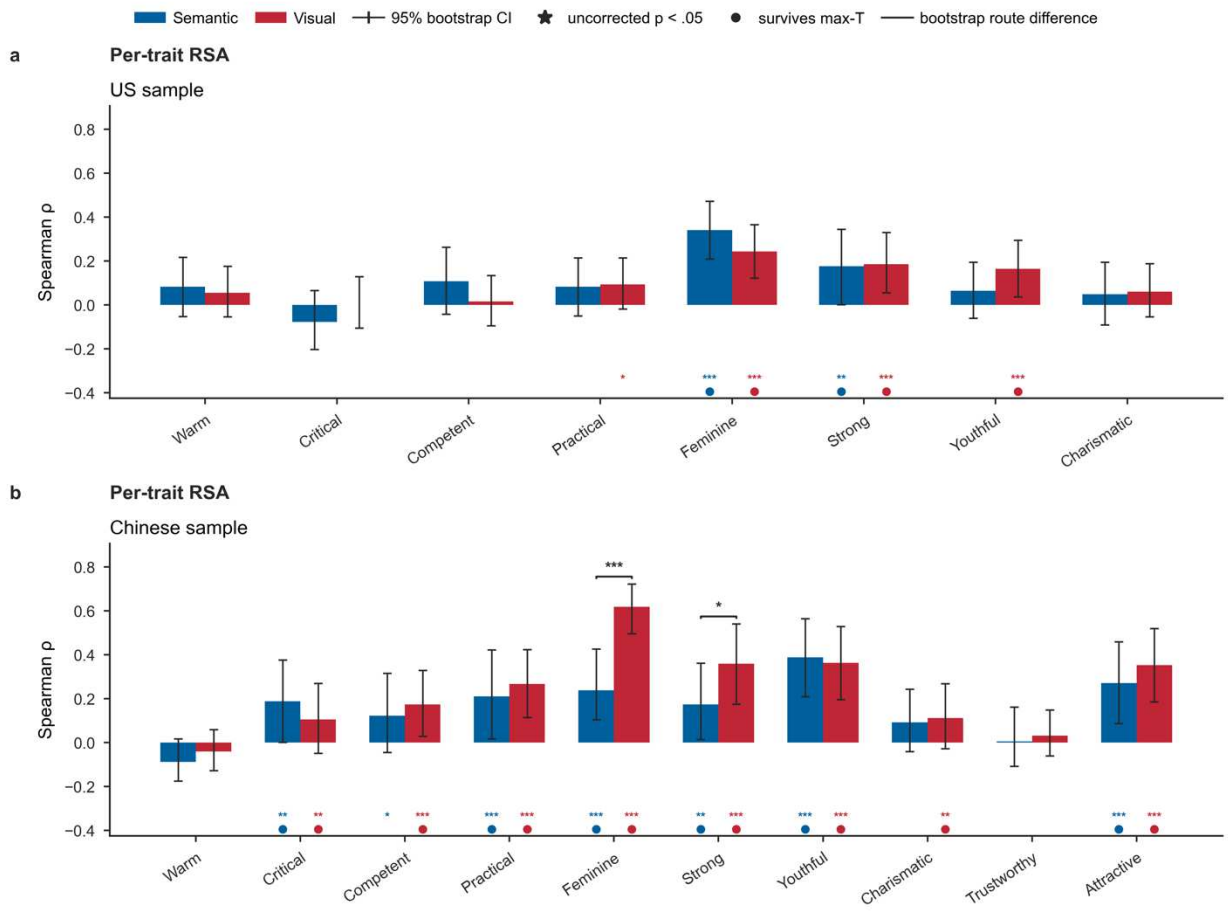


Figure 6. Correlations between individual social trait spaces and visual/semantic spaces: (a) U.S. sample; (b) Chinese sample. Blue and red asterisks indicate statistical significance level of the association between the social trait RDM and the semantic RDM (blue) and visual RDM (red) by permutation; a filled dot marks associations that additionally survive max-T correction within channel and dataset. Error bars are 95% confidence intervals from the bootstrap, and black

brackets mark traits whose two routes differ in that same bootstrap. *: < .05, **: < .01, ***: < .001.

For the Chinese data, semantic information was significantly associated with seven of the ten trait impressions: youthfulness (ρ = .39, p_{perm} < .001), attractiveness (ρ = .27, p_{perm} < .001), femininity (ρ = .24, p_{perm} < .001), practicalness (ρ = .21, p_{perm} < .001), criticalness (ρ = .19, p_{perm} = .003), physical strength (ρ = .17, p_{perm} = .003), and competence (ρ = .12, p_{perm} = .012), as shown in **Figure 6**. On the other hand, the visual model was significantly correlated with eight of the ten dimensions: femininity (ρ = .62, p_{perm} < .001), physical strength (ρ = .36, p_{perm} < .001), youthfulness (ρ = .36, p_{perm} < .001), attractiveness (ρ = .35, p_{perm} < .001), practicalness (ρ = .27, p_{perm} < .001), competence (ρ = .17, p_{perm} < .001), criticalness (ρ = .11, p_{perm} = .007), and charisma (ρ = .11, p_{perm} = .004). Comparing the routes, visual information was more strongly associated with femininity ($\Delta\rho$ = −.38 [−.51, −.22], p_{boot} < .001) and physical strength ($\Delta\rho$ = −.19 [−.36, −.02], p_{boot} = .029) than semantic information.

After correcting for multiple comparisons with max-T permutation tests, which control the family-wise error rate (*k = 5,000*; family = all traits per model per dataset), in the U.S. sample (eight trait models), the associations surviving correction (p_{maxt} < .05) were femininity (ρ = .34, p_{maxt} < .001) and physical strength (ρ = .18, p_{maxt} = .028) for the semantic model, and femininity (ρ = .24, p_{maxt} < .001), physical strength (ρ = .19, p_{maxt} < .001), and youthfulness (ρ = .16, p_{maxt} = .001) for the visual model. In the Chinese sample (10 trait models), criticalness (ρ = .19, p_{maxt} = .012), practicalness (ρ = .21, p_{maxt} = .005), femininity (ρ = .24, p_{maxt} = .002), physical strength (ρ = .17, p_{maxt} = .020), youthfulness (ρ = .39, p_{maxt} < .001), and attractiveness (ρ = .27, pmaxt < .001) survived for the semantic model; criticalness (ρ = .11, p_{maxt} = .046), competence (ρ = .17, p_{maxt} = .002), practicalness (ρ = .27, p_{maxt} < .001), femininity (ρ = .62, p_{maxt}

< .001), physical strength (ρ = .36, p_{maxt} < .001), youthfulness (ρ = .36, p_{maxt} < .001), charisma (ρ = .11, p_{maxt} = .030), and attractiveness (ρ = .35, p_{maxt} < .001) survived for the visual model. Full model statistics are reported in the **Table S1**.

Overall, the findings support H1 that both the perceptual and conceptual routes were associated with facial trait impressions, especially for multidimensional trait-spaces in both samples. At the individual-trait level, the results further showed that the pattern was trait-specific and dataset dependent. In the U.S. sample, both routes were associated with a smaller set of traits, especially femininity, and physical strength. In the Chinese sample, both routes were associated with a broader range of trait representations, including femininity, physical strength, criticalness, practicalness, youth and attractiveness. Together, these findings indicate that facial trait impressions are organized by both visual facial information and conceptual knowledge, while also showing that the strength of each route varies across traits and datasets.

Both routes explain unique variance in trait impression formation (H2)

The above RSA treats each route in isolation, to further test whether visual and semantic information has unique and shared contributions to social trait impression, we conducted variance partitioning analyses, testing the significance of each unique contribution by permuting target labels and using bootstrapping over targets for confidence intervals and route comparisons (see *Methods: Analysis*).

Before partitioning variance between the two routes, we examined the extent to which the visual and semantic model RDMs were separable. The semantic and visual RDMs were weakly correlated in the U.S. sample (ρ = .17, r = .18, 3.3% shared variance) and modestly correlated in the Chinese sample (ρ = .34, r = .37, 14.0% shared variance). There is no problematic multicollinearity between the two routes: variance inflation factors (VIF) for the two-predictor regression never exceeded 1.03 in the U.S. sample or 1.16 in the Chinese sample, well below any conventional threshold of 5 or 10. We therefore proceeded to variance partitioning to estimate the unique and shared contributions of the visual and semantic routes.

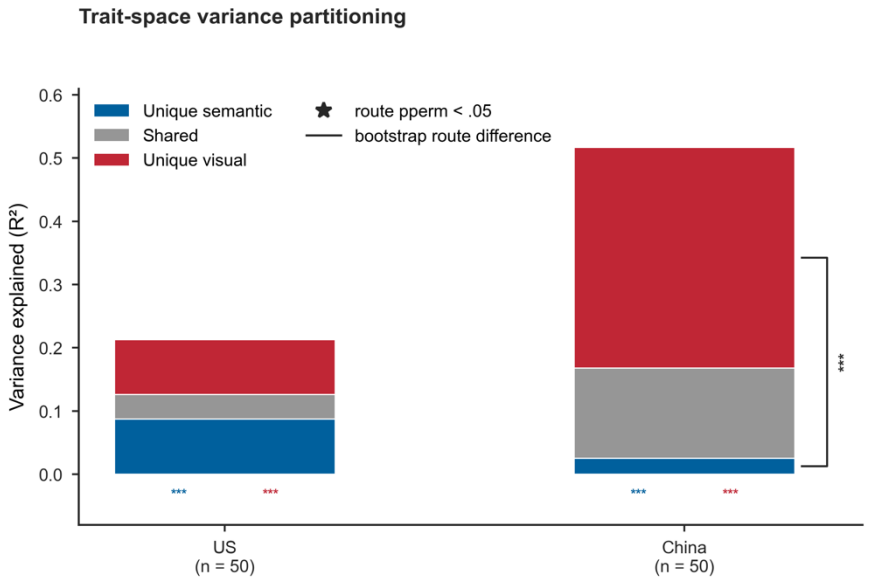


Figure 7. Trait-space variance partitioning: unique and shared contributions of the semantic and visual RDMs to the multidimensional social trait RDM in the (a) U.S. and (b) Chinese samples. Colored asterisks below the bars indicate significant unique contributions p_{perm} based on permutation tests of target labels: unique semantic contribution (blue) and unique visual contribution (red). A vertical bracket beside a bar indicates a significant level of difference between the two routes' unique contributions based on the paired identity-level bootstrap p_{boot}. *: < .05, **: < .01, ***: < .001.

At the level of the multidimensional trait space (**Figure 7**), both routes explained significant unique variance in both datasets. In the U.S. sample the semantic route uniquely explained ΔR^2 = 8.7% [2.7, 18.7], $p_{perm} < .001$ and the visual route ΔR^2 = 8.7% [2.5, 18.5], $p_{perm} < .001$, and the two did not differ significantly ($\Delta\Delta R^2$ = 0.1% [-14.2, 14.4], p_{boot} = .934). Similarly in the Chinese sample, both the semantic route (ΔR^2 = 2.5% [0.2, 7.4], $p_{perm} < .001$) and the visual route (ΔR^2 = 34.9% [24.1, 46.0], $p_{perm} < .001$) explained significant unique variance in trait impression. The semantic route therefore contributes to trait impression that cannot be explained by the visual model. Interestingly, the variance explained by the visual route was significantly larger than the variance explained by the semantic route ($\Delta\Delta R^2$ = -32.3% [-45.3, -17.6], $p_{boot} < .001$).

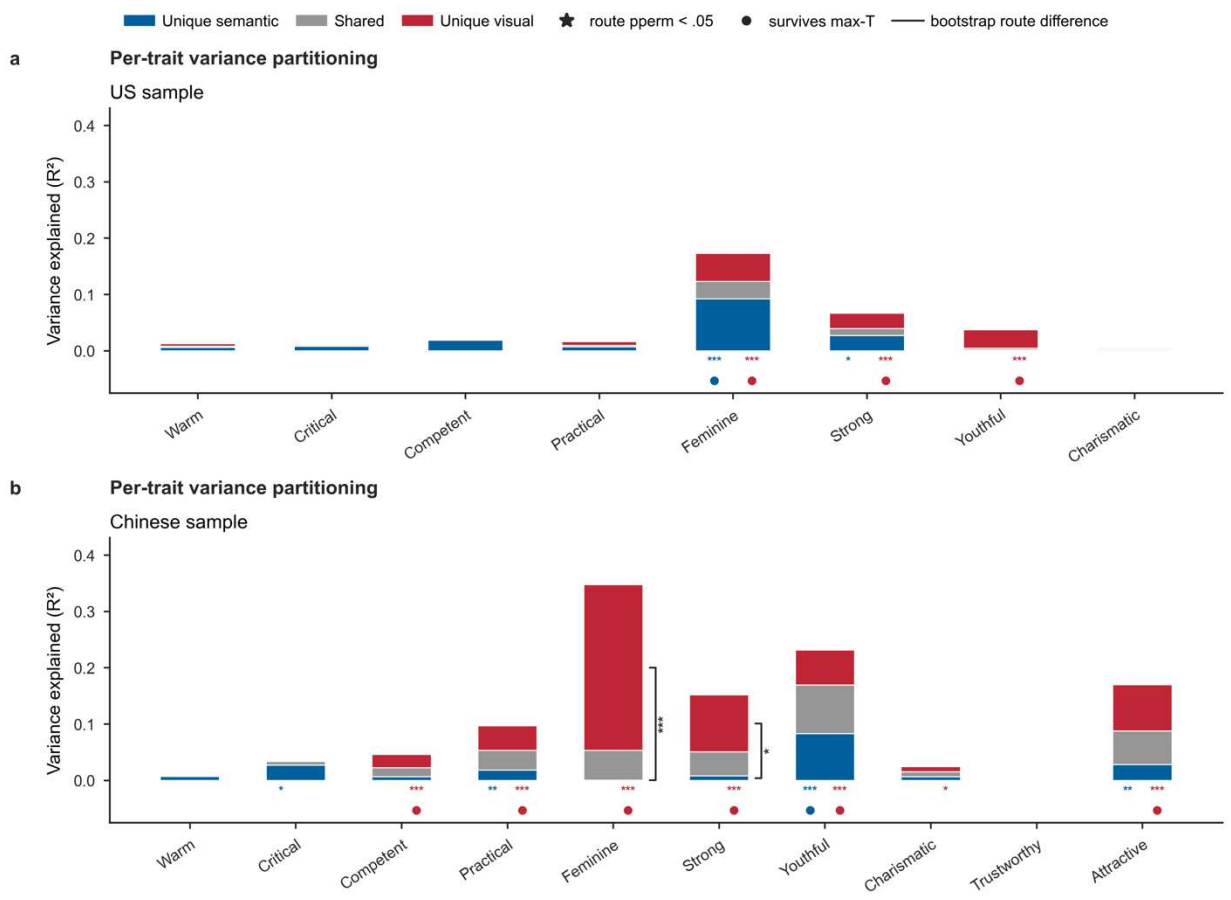


Figure 8. Variance partitioning of the unique and shared contributions of visual and semantic RDMs to individual social-trait RDMs in the (a) U.S. sample and (b) Chinese sample. Bars show the unique variance explained by each route, and shared variance. Colored asterisks below the bars indicate significant unique contributions p_{perm} based on permutation tests of target labels; dots mark those that additionally survive max-T family-wise correction within channel and dataset $p_{maxt} < .05$: unique semantic contribution (blue) and unique visual contribution (red). A vertical bracket beside a bar indicates a significant level of difference between the two routes' unique contributions based on the paired identity-level bootstrap p_{boot}. *: < .05, **: < .01, ***: < .001.

For the individual traits in the U.S. data, the unique contribution of semantic information (the blue portion of the bars in **Figure 8**) was significant for femininity (ΔR^2 = 9.2% [3.1, 18.9], $p_{perm} < .001$) and physical strength (ΔR^2 = 2.7% [0.0, 10.2], p_{perm} = .019); competence (ΔR^2 = 1.9% [0.0, 9.1], p_{perm} = .076), criticalness (ΔR^2 = 0.9% [0.0, 5.6], p_{perm} = .157), practicalness (ΔR^2 = 0.7% [0.0, 5.0], p_{perm} = .245) and warmth (ΔR^2 = 0.6% [0.0, 5.5], p_{perm} = .202) did not reach significance. The unique contribution of visual information (the red portion of the bars) was significant for femininity (ΔR^2 = 5.0% [0.8, 12.1], $p_{perm} < .001$), physical strength (ΔR^2 = 2.7% [0.2, 8.3], $p_{perm} < .001$), and youthfulness (ΔR^2 = 3.3% [0.4, 9.3], $p_{perm} < .001$), while the contribution for practicalness (ΔR^2 = 0.6% [0.0, 3.9], p_{perm} = .055) and warmth (ΔR^2 = 0.5% [0.0, 3.8], p_{perm} = .085) was marginally significant. Reliable unique contributions in the U.S. sample were thus confined to the most physically grounded traits. The visual and semantic unique contributions did not differ significantly for any trait.

For the Chinese data, the semantic information explained significant unique variance in 4 of the 10 trait dimensions: youthfulness (ΔR^2 = 8.3% [2.4, 16.4], $p_{perm} < .001$), attractiveness (ΔR^2 = 2.8% [0.1, 10.0], p_{perm} = .009), practicalness (ΔR^2 = 1.8% [0.0, 10.0], p_{perm} = .008), and criticalness (ΔR^2 = 2.7% [0.0, 11.2], p_{perm} = .017), indicating that conceptual knowledge contributed to trait impressions even when the participants were asked to rate impressions based on faces. The contributions to competence (ΔR^2 = 0.7% [0.0, 5.5], p_{perm} = .142), warmth (ΔR^2 = 0.7% [0.0, 3.6], p_{perm} = .178), physical strength (ΔR^2 = 0.8% [0.0, 4.9], p_{perm} = .184) and charisma (ΔR^2 = 0.6% [0.0, 4.6], p_{perm} = .234) were not significant, and neither were those to femininity or trustworthiness. The visual model explained significant unique variance in 7 of the 10 dimensions, most strongly for femininity (ΔR^2 = 29.4% [18.4, 41.2], $p_{perm} < .001$), physical strength (ΔR^2 = 10.1% [2.8, 21.4], $p_{perm} < .001$), attractiveness (ΔR^2 = 8.2% [1.8, 18.4], p_{perm}

< .001), and youthfulness (ΔR^2 = 6.2% [1.1, 15.1], p_{perm} < .001), and also for practicalness (ΔR^2 = 4.4% [0.5, 13.0], p_{perm} < .001), competence (ΔR^2 = 2.4% [0.1, 8.3], p_{perm} < .001), and charisma (ΔR^2 = 0.9% [0.0, 5.7], p_{perm} = .033); criticalness, trustworthiness and warmth were not significant (all p_{perm} > .05). Comparing the two routes directly, the visual model dominated over the semantic model for femininity ($\Delta\Delta R^2$ = -29.4% [-40.9, -17.5], p_{boot} < .001) and physical strength ($\Delta\Delta R^2$ = -9.3% [-20.6, -0.4], p_{boot} = .039).

To correct for multiple comparisons, we then corrected the individual-trait unique contributions with a max-T permutation procedure over the same 5,000 permutations, controlling the family-wise error rate within each channel and each dataset (family = all traits per channel per dataset). In the U.S. sample the surviving semantic contribution was femininity (ΔR^2 = 9.2%, p_{maxt} < .001), and the surviving visual contributions were femininity, physical strength, youthfulness (femininity ΔR^2 = 5.0%, p_{maxt} < .001; physical strength ΔR^2 = 2.7%, p_{maxt} < .001; youthfulness ΔR^2 = 3.3%, p_{maxt} < .001); the semantic contribution to physical strength did not survive (ΔR^2 = 2.7%, p_{maxt} = .106). In the Chinese sample the surviving semantic contribution was youthfulness (ΔR^2 = 8.3%, p_{maxt} < .001), with criticalness (ΔR^2 = 2.7%, p_{maxt} = .068) and attractiveness (ΔR^2 = 2.8%, p_{maxt} = .061) trending, and six visual contributions survived including competence, practicalness, femininity, physical strength, youthfulness, attractiveness. Full model statistics are reported in the **Table S2**.

Together, these findings provide support for H2 at the level of the multidimensional trait space and a subset of individual traits. Physical and semantic information each accounted for distinct variance in participants' judgments. Trait impressions of public figures therefore appear

to arise from a dual-route process, integrating visual information from facial appearance with person-specific semantic knowledge about the target.

Familiarity modulates the visual and semantic contributions to social trait impressions (H3)

An implication of the dual-route model is that familiarity with the target should modulate the visual and conceptual contributions to social trait impressions. Familiarity provides an observational moderation test because participants may differ in their familiarity with particular celebrities, allowing us to examine whether route reliance covaries with naturally occurring differences in person knowledge. Here, familiarity was modeled at the perceiver × target level, capturing trial-level variation in each perceiver's familiarity with each target. At the trait-space level (**Figure 9**), familiarity moderated the semantic route in the Chinese sample: greater familiarity with a pair was associated with increased association between the perceiver's trait profile distances and the semantic model (β = .023 [.006, .039], p = .007), partly supporting H3. The visual route did not reach significance (β = .012 [−.001, .025], p = .073). In the U.S. sample neither route was moderated by recognition (semantic β = .005 [−.011, .020], p = .563; visual β = −.001 [−.016, .013], p = .854). Because the trait space is a single outcome by construction, these tests carry no multiple-comparison family.

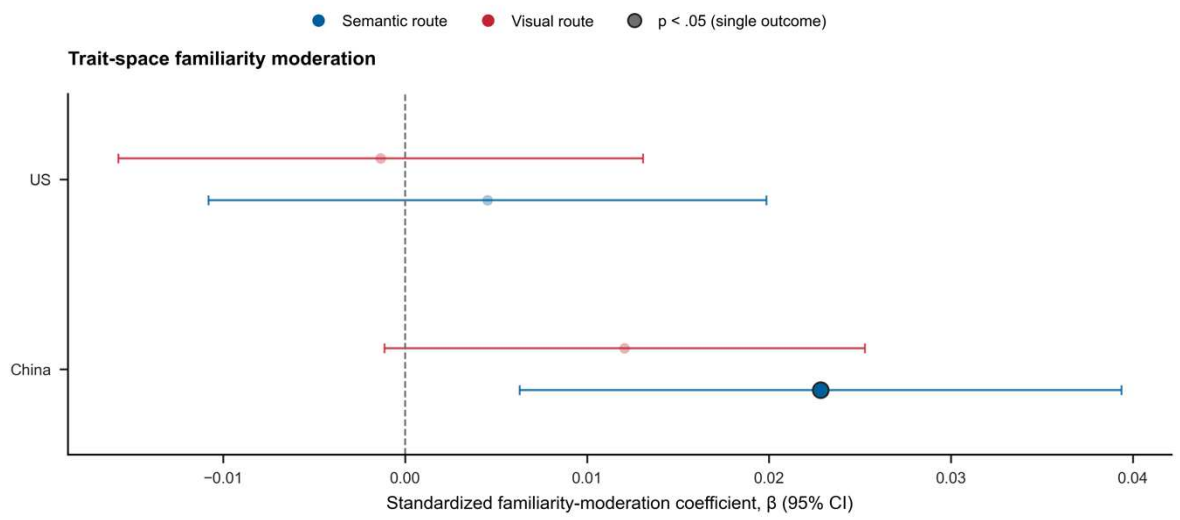


Figure 9. Trait-space linear mixed model: moderation of the semantic and visual effects by perceiver-level familiarity (Chinese sample) or recognition (U.S. sample). Points show interaction betas (semantic × familiarity in blue; visual × familiarity in red) with 95% confidence intervals; the filled dot indicates $p < .05$. Because the trait space is a single outcome, no multiple comparison family applies.

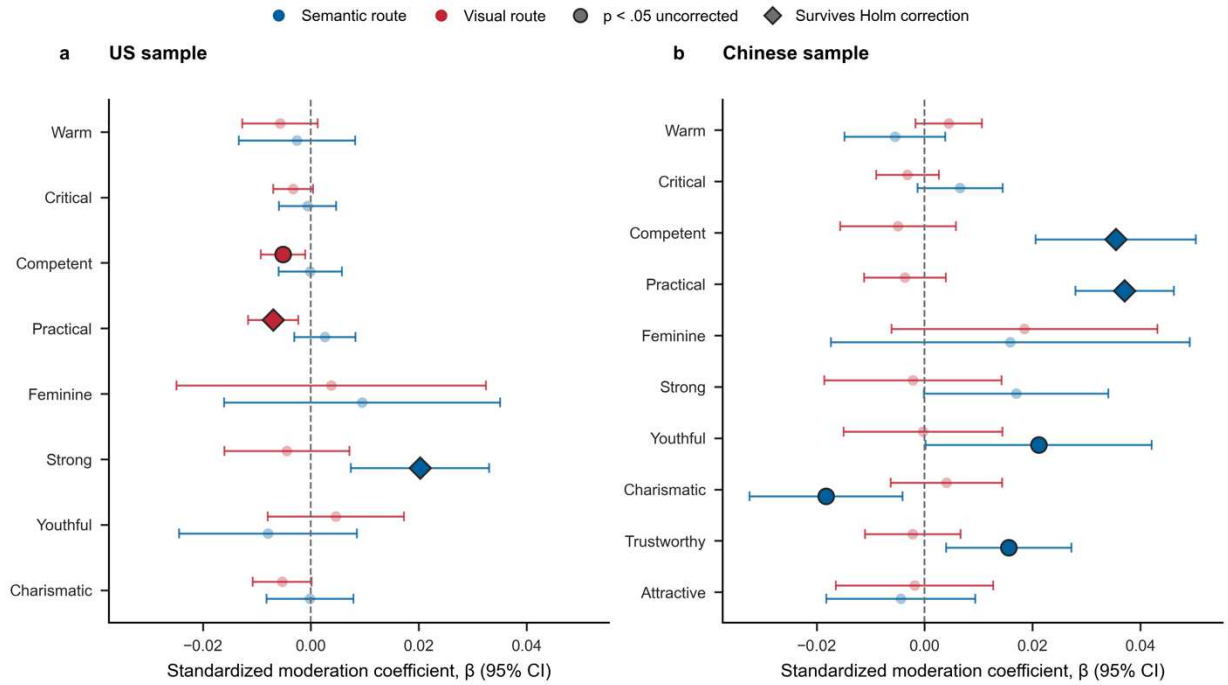


Figure 10. Familiarity moderation of the semantic and visual associations with each trait impression in the (a) U.S. sample and (b) Chinese sample. Dots indicate interaction betas (semantic × familiarity in blue; visual × familiarity in red) with 95% confidence intervals; filled circles indicate effects significant at $p < .05$ before correction, and diamonds indicate effects that survived Holm correction across traits.

For the U.S. data, familiarity was operationalized as recognition, because participants only indicated binarily whether they recognize a given celebrity or not. We found that recognition moderated the routes to trait impressions, but the pattern was trait-specific (**Figure 10**). Recognized targets relied less on visual information for practicalness ($\beta = -.007$ [−.012, −.002], $p = .003$) and competence ($\beta = -.005$ [−.009, −.001], $p = .014$), and relied more on semantic information for physical strength ($\beta = .020$ [.007, .033], $p = .002$).

For the Chinese data, familiarity, measured on Likert scale (1 = not recognize, 7 = extremely familiar), more consistently moderated the semantic route. The Semantic × Familiarity interaction was significantly positive for five traits (**Figure 10)**: practicalness ($\beta = .037$ [.028, .046], $p < .001$), competence ($\beta = .035$ [.021, .050], $p < .001$), the trait space, trustworthiness ($\beta = .016$ [.004, .027], $p = .008$) and youthfulness ($\beta = .021$ [.000, .042], $p = .048$). For these outcomes, greater familiarity with a pair of targets was associated with stronger alignment between semantic distance and trait distance between the two target. The only significantly negative modulation of familiarity was the Semantic × Familiarity interaction for charisma ($\beta = -.018$ [−.032, −.004], $p = .012$). Thus, although the heterogeneity in moderation effects suggests that familiarity does not modulate semantic and visual weights in the same way across all traits, the results largely supported H3.

We then applied Holm–Bonferroni correction within each dataset and channel. In the U.S. sample, the Semantic × Recognition effect for physical strength (p_{Holm} = .016) and the Visual × Recognition effect for practicalness (p_{Holm} = .026) remained significant. The Visual × Recognition effect for competence did not survive correction (p_{Holm} = .097). In the Chinese sample, two Semantic × Familiarity effects survived correction: practicalness (p_{Holm} < .001) and competence (p_{Holm} < .001). The positive effect for trustworthiness (p_{Holm} = .067) and the negative effect for charisma (p_{Holm} = .081) did not survive correction. Full model statistics are reported in the Supplementary Materials (Table S3). Thus, the main pattern survived family-wise support for at least one trait in each dataset, with more evidence emerging for semantic amplification in the Chinese sample.

Together, these findings provide support for the central prediction of H3. In the Chinese dataset, familiarity generally amplified the contribution of semantic knowledge to social-trait impressions, especially for practicalness and competence. In the U.S. dataset, recognition showed a more selective pattern: after correction, it increased semantic alignment for physical strength and reduced visual alignment for practicalness; a nominally similar reduction for competence did not survive correction. Thus, although familiarity did not uniformly increase semantic contributions across all traits, the overall pattern suggests that better-known targets are more likely to recruit semantic information in trait-specific ways.

Discussion

In this study, we proposed and tested a dual-route model of facial trait impressions across two datasets of facial trait impressions of Western and East Asian celebrities. The model posits

that both perceptual information of the face and conceptual knowledge about the person contribute to social trait impressions. Consistent with H1, we found that both visual and semantic routes were associated with the structure of trait impressions. At the individual-trait level, the associations that survived family-wise error control in the U.S. sample were concentrated in perceptually grounded traits. The visual model significantly tracked femininity, physical strength, and youthfulness, whereas the semantic model significantly tracked femininity and physical strength. In the Chinese sample, corrected associations were broader: both models tracked femininity, physical strength, youthfulness, attractiveness, practicalness, and criticalness, and the visual model additionally tracked competence and charisma. Consistent with H2, the two routes made unique contributions to trait impressions. Each model explained significant unique variance in the multidimensional trait spaces, again with similar contributions in the U.S. sample and significantly dominant visual contribution in the Chinese sample.

The dual-route framework of trait impressions both confirms and complements the appearance-based account of impressions (Oosterhof & Todorov, 2008; Todorov et al., 2015). Consistent with appearance-based accounts, the visual route dominated the multidimensional trait space and several physically grounded traits in the Chinese sample. The visual representational structure was more strongly associated with femininity and physical strength and, in variance partitioning, showed larger unique contributions to the facial trait impression structure in the Chinese sample. The account is incomplete, however, for the broader set of traits. Practicalness, criticalness, and others carried reliable semantic structure beyond the visual model, indicating that even rapid trait impressions of real people incorporate conceptual knowledge. The appearance-based account was built on unfamiliar faces, which by design ignored the conceptual

route; when the targets are people about whom the perceiver knows or infers something, that route becomes substantial.

The findings also build on the dynamic-interactive account of person construal (Freeman & Ambady, 2011) and representational approach of trait impressions (Brooks & Freeman, 2018; Stolier et al., 2018, 2020). The dual-route approach extends this program in two ways. First, we decompose trait impressions with an image-based perceptual model and a text-based, target-specific conceptual model, allowing us to estimate each route's unique and shared variance on a common scale. This approach is also transferable beyond images and text: additional routes could be instantiated with other modalities, such as vocal information represented by audio models, allowing future work to ask how visual, verbal, auditory, and other social signals jointly contribute to impression formation. More broadly, the findings suggest that traits are not intrinsically visual or semantic. A given trait impression may draw on whichever source of information carries the most diagnostic signal in a particular stimulus set, cultural or social contexts, and perceiver population. The dual-route framework therefore offers a more flexible account of person perception: faces provide an entry point for social evaluation, but impressions of real people emerge from the interaction between what is visible in the face and what is known about the person.

Second, whereas much prior work has related perceiver-level conceptual structure to impression structure or modeled social categorization, the conceptual side of the previous framework has largely concerned general conceptual structure such as group-level stereotypes (Stolier et al., 2018; Xie et al., 2021), top-down social-category knowledge (Freeman & Ambady, 2011), perceivers' idiosyncratic beliefs about trait covariation (Hehman et al., 2017; Stolier et al., 2018, 2020). This distinction is important because it shifts the conceptual route

from a general belief system about traits or groups to knowledge about particular people. In everyday social life, perceivers rarely judge completely anonymous faces. Instead, faces are often attached to names, reputations, social roles, prior encounters, and culturally shared narratives. The present findings suggest that these target-specific semantic representations can contribute to the structure of facial trait impressions above and beyond visual appearance.

The familiarity findings further support this argument. Familiarity selectively enhances the conceptual route for some traits while leaving the visual route unchanged. This pattern suggests that familiarity does not simply increase the use of all available information; instead, it changes which route is most diagnostic for a given trait. For traits such as competence and practicalness, familiar targets may evoke knowledge about occupations, accomplishments, public behavior, and social roles, making semantic representations especially informative. For traits more directly tied to visible appearance, such as femininity or youthfulness, visual information may remain highly diagnostic regardless of familiarity. The route carrying a trait is therefore not fixed; it depends on which source of information carries the more reliable trait-relevant signal in a given dataset and perceiver population. Theoretically, these findings suggest that social perception is neither a series of isolated visual snapshots nor a simple accumulation of repeated exposures; what a perceiver already knows about a target can update which sources of information are weighted more strongly in forming an impression (Jain & Schiller, 2026).

Why does greater familiarity weaken the semantic route for charisma? One possibility is that this effect reflects what our semantic model captures. Our semantic space was built from aggregate public text and therefore indexes public, broadly shared knowledge about a target, rather than the private, idiosyncratic knowledge that a particular perceiver accumulates through their personal experience. On this account, familiarity may not weaken the conceptual route

itself. Instead, its basis may shift from public semantic knowledge toward more private knowledge. Charisma may be especially sensitive to this shift because it is often judged from dynamic, affective, and interaction-like cues that are only partially represented in encyclopedic text. As impressions become increasingly grounded in individualized forms of knowledge, a public semantic model may fit those impressions less well, producing the negative familiarity interaction for charisma. In this way, familiarity may increase reliance on conceptual knowledge, but the relevant conceptual knowledge may be private rather than publicly represented in media text. Future research should directly measure perceiver-specific knowledge about targets and test whether individualized semantic representations explain trait impressions beyond public semantic models.

Overall, the results support a dual-route account of facial trait impressions. Facial appearance and person knowledge both contribute to trait impressions, and each explains variance that the other does not. Familiarity further shifts this balance, mostly by amplifying semantic contributions for knowledge-dependent traits. These findings suggest that impressions made from faces are not determined by appearance alone. Instead, the same face can carry multiple information routes, including what is visually available in the image and what is conceptually known about the person.

Our current studies have several limitations. First, as aforementioned, our semantic model captures shared, public knowledge, not any individual perceiver's actual knowledge. Establishing the effect of familiarity on the private conceptual contribution to trait impressions would require per-perceiver measures of what each individual knows about each target. Second, the two datasets differed by design in target familiarity and measurement resolution: the U.S. sample involved predominantly fewer familiar targets and binary familiarity ratings, whereas the

Chinese sample involved more familiar targets and a more granular familiarity measure, providing greater sensitivity. Relatedly, familiarity was measured rather than manipulated and more familiar targets tend to differ systematically in occupation, age and popularity. These differences mean that the two datasets are not directly comparable. Moreover, dataset differences should not be interpreted as cultural differences because the structure of social impressions varies across world regions and perceiver characteristics rather than mapping onto fixed cultural categories (Oh et al., 2022). Third, celebrities are a particular kind of known target, and the conceptual knowledge perceivers hold about public figures may differ from knowledge of personal acquaintances; generalization to everyday familiarity remains to be tested (Ramon & Gobbini, 2018). Finally, although we selected models that were theoretically motivated and well suited to our research question, the estimated contributions of the visual and semantic routes may vary with alternative model choices. Rather than treating this as a model dependence, future work could use the current work as a benchmarking approach, comparing different vision, language, and multimodal models to test which representations best capture trait impressions.

These limitations also point to future directions. The dual-route framework provides a way to move beyond investigating whether visual appearance or conceptual knowledge matters for impressions, toward examining which representations matter, for which traits, and under what social conditions. Future work could combine public semantic models with direct measures of perceiver-specific private knowledge, systematically vary target familiarity within the same sample, and extend the framework to other ecologically important signals, such as voices, bodies, behavior, and interaction histories. Such work would help determine when impressions are captured in shared public representations, when they are shaped by private person

knowledge, and how different sources of social information are integrated as people become known.

Conclusion

To conclude, our study tested a dual-route of facial trait impressions and shows that facial trait impressions are shaped by both visual appearance and person-specific conceptual knowledge about the target, with each route contributing unique variance. Familiarity shifts this balance toward semantic knowledge, especially for knowledge-dependent traits. Together, these findings provide a representational framework for quantifying how perception and knowledge jointly shape social trait impressions, and for examining how that weighting changes across traits, targets, perceivers, and social contexts.

Data Availability. https://github.com/amberxuqianchen/dual-route-traits-osf

Author Contributions (CRediT). Chen: Conceptualization, Methodology, Software, Formal Analysis, Investigation, Visualization, Writing – Original Draft, and Writing – Review & Editing. Liu: Investigation, Data Curation, Project Administration, Formal Analysis, Writing – Original Draft, and Writing – Review & Editing. Zhao: Supplementary Analysis and Writing – Review & Editing. Ma de Sousa: Writing – Review & Editing. Peng: Resources, Supervision, Project Administration, Funding Acquisition, and Writing – Review & Editing. Yu: Conceptualization, Methodology, Supervision, and Writing – Review & Editing. All authors approved the final version of the manuscript.

Conflict of Interest. The authors declare no competing interests.

Funding. [Placeholder — grant numbers / "no funding".]

AI-Use Disclosure. The authors used ChatGPT (versions 5.5 and 5.6) to assist with language editing, manuscript polishing, organization of selected materials, and improvement of clarity and structure during manuscript preparation. Claude Code (Opus 5 and Sonnet 5) was used to assist with coding, debugging, and organization of analysis scripts. In addition, a pretrained VGGFace2-based vision model and an OpenAI embedding model were used as part of the analytic pipeline to derive visual and semantic representations, respectively. AI tools were not used to generate hypotheses, collect participant data, conduct unsupervised analyses, or make scientific decisions. All AI-assisted outputs, including organized materials, edited text, code, visual embeddings, and semantic embeddings, were reviewed, verified, and interpreted by the authors. The authors take full responsibility for the accuracy, integrity, and final content of the manuscript.

References

Abele, A. E., Hauke, N., Peters, K., Louvet, E., Szymkow, A., & Duan, Y. (2016). Facets of the Fundamental Content Dimensions: Agency with Competence and Assertiveness—Communion with Warmth and Morality. *Frontiers in Psychology, 0*. https://doi.org/10.3389/fpsyg.2016.01810

Abele, A. E., & Wojciszke, B. (2014). Communal and agentic content in social cognition: A dual perspective model. *Advances in Experimental Social Psychology*, *50*, 195–255.

Amodio, D. M. (2025). A learning and memory account of impression formation and updating. *Nature Reviews Psychology*, 1–16. https://doi.org/10.1038/s44159-025-00445-x

Barr, D. J., Levy, R., Scheepers, C., & Tily, H. J. (2013). Random effects structure for confirmatory hypothesis testing: Keep it maximal. *Journal of Memory and Language*, *68*(3). https://doi.org/10.1016/j.jml.2012.11.001

Brewer, M. B. (1988). A dual process model of impression formation. In *A dual process model of impression formation* (pp. 1–36). Lawrence Erlbaum Associates, Inc.

Brooks, J. A., & Freeman, J. B. (2018). Conceptual knowledge predicts the representational structure of facial emotion perception. *Nature Human Behaviour*, *2*(8), Article 8. https://doi.org/10.1038/s41562-018-0376-6

Brooks, M. E., Kristensen, K., van Benthem, K. J., Magnusson, A., Berg, C. W., Nielsen, A., Skaug, H. J., Maechler, M., & Bolker, B. M. (2017). glmmTMB balances speed and flexibility among packages for zero-inflated generalized linear mixed modeling. *The R Journal, 9*(2), 378–400. https://doi.org/10.32614/RJ-2017-066

Burton, A. M., Kramer, R. S. S., Ritchie, K. L., & Jenkins, R. (2016). Identity From Variation: Representations of Faces Derived From Multiple Instances. *Cognitive Science*, *40*(1),

202–223. https://doi.org/10.1111/cogs.12231

Cao, Q., Shen, L., Xie, W., Parkhi, O. M., & Zisserman, A. (2018). *VGGFace2: A dataset for recognising faces across pose and age* (arXiv:1710.08092). arXiv. https://doi.org/10.48550/arXiv.1710.08092

Cao, R., Zhang, N., Yu, H., Webster, P. J., Paul, L. K., Li, X., Lin, C., & Wang, S. (2023). Comprehensive Social Trait Judgments From Faces in Autism Spectrum Disorder. *Psychological Science*, *34*(10), 1121–1145. https://doi.org/10.1177/09567976231192236

Cao, X., & Kosinski, M. (2024). Large language models know how the personality of public figures is perceived by the general public. *Scientific Reports*, *14*(1), 6735. https://doi.org/10.1038/s41598-024-57271-z

Charest, I., Kievit, R. A., Schmitz, T. W., Deca, D., & Kriegeskorte, N. (2014). Unique semantic space in the brain of each beholder predicts perceived similarity. *Proceedings of the National Academy of Sciences*, *111*(40), 14565–14570. https://doi.org/10.1073/pnas.1402594111

Chen, A. X., Sun, S., & Yu, H. (2024). Moral attitudes towards effort and efficiency: A comparison between American and Chinese history. *Humanities and Social Sciences Communications*, *11*(1), 1–14. https://doi.org/10.1057/s41599-024-03603-3

Chua, K.-W., & Freeman, J. B. (2021). Facial stereotype bias is mitigated by training. *Social Psychological and Personality Science*, *12*(7), 1335–1344. https://doi.org/10.1177/1948550620972550

Cone, J., Mann, T. C., & Ferguson, M. J. (2017). Changing Our Implicit Minds: How, When, and Why Implicit Evaluations Can Be Rapidly Revised. In *Advances in Experimental Social Psychology* (Vol. 56, pp. 131–199). Elsevier.

https://doi.org/10.1016/bs.aesp.2017.03.001

Connor, P., Nicolas, G., Antonoplis, S., & Koch, A. (2024). Unconstrained Descriptions of Facebook Profile Pictures Support High-Dimensional Models of Impression Formation. *Personality & Social Psychology Bulletin*, 1461672241266651. https://doi.org/10.1177/01461672241266651

Cook, R., Eggleston, A., & Over, H. (2022). The cultural learning account of first impressions. *Trends in Cognitive Sciences*, *26*(8), 656–668. https://doi.org/10.1016/j.tics.2022.05.007

Dobs, K., Yuan, J., Martinez, J., & Kanwisher, N. (2023). Behavioral signatures of face perception emerge in deep neural networks optimized for face recognition. *Proceedings of the National Academy of Sciences of the United States of America*, *120*(32), e2220642120. https://doi.org/10.1073/pnas.2220642120

FeldmanHall, O., Dunsmoor, J. E., Tompary, A., Hunter, L. E., Todorov, A., & Phelps, E. A. (2018). Stimulus generalization as a mechanism for learning to trust. *PNAS Proceedings of the National Academy of Sciences of the United States of America*, *115*(7), E1690–E1697. https://doi.org/10.1073/pnas.1715227115

Fiske, S. T., Cuddy, A. J. C., & Glick, P. (2007). Universal dimensions of social cognition: Warmth and competence. *Trends in Cognitive Sciences*, *11*(2), 77–83. https://doi.org/10.1016/j.tics.2006.11.005

Fiske, S. T., & Neuberg, S. L. (1990). *A continuum of impression formation, from category-based to individuating processes: Influences of information and motivation on attention and interpretation* (M. P. Zanna, Ed.; Vol. 23, pp. 1–74). Academic Press. https://doi.org/https://doi.org/10.1016/S0065-2601(08)60317-2

Freeman, J. B., & Ambady, N. (2011). A dynamic interactive theory of person construal.

Psychological Review, *118*(2), 247–279. https://doi.org/10.1037/a0022327

Freeman, J. B., & Chwe, J. A. (2024). Social Categorization: Looking Toward the Future. In D. E. Carlston, K. Hugenberg, & K. L. Johnson (Eds.), *The Oxford Handbook of Social Cognition, Second Edition* (2nd ed., pp. 198–221). Oxford University Press. https://doi.org/10.1093/oxfordhb/9780197763414.013.7

Freeman, J. B., & Lin, C. (2025). A high-dimensional model of social impressions. *Trends in Cognitive Sciences*, *0*(0). https://doi.org/10.1016/j.tics.2025.04.011

Freeman, J. B., Stolier, R. M., & Brooks, J. A. (2020). Dynamic interactive theory as a domain-general account of social perception. In *Advances in Experimental Social Psychology* (Vol. 61, pp. 237–287). Elsevier. https://doi.org/10.1016/bs.aesp.2019.09.005

Geniole, S. N., Molnar, D. S., Carré, J. M., & McCormick, C. M. (2014). The facial width-to-height ratio shares stronger links with judgments of aggression than with judgments of trustworthiness. *Journal of Experimental Psychology: Human Perception and Performance*, *40*(4), 1526–1541. https://doi.org/10.1037/a0036732

Gobbini, M. I., & Haxby, J. V. (2007). Neural systems for recognition of familiar faces. *Neuropsychologia*, *45*(1), 32–41. https://doi.org/10.1016/j.neuropsychologia.2006.04.015

Grand, G., Blank, I. A., Pereira, F., & Fedorenko, E. (2022). Semantic projection recovers rich human knowledge of multiple object features from word embeddings. *Nature Human Behaviour*, *6*(7), 975–987. https://doi.org/10.1038/s41562-022-01316-8

Groen, I. I., Greene, M. R., Baldassano, C., Fei-Fei, L., Beck, D. M., & Baker, C. I. (2018). Distinct contributions of functional and deep neural network features to representational similarity of scenes in human brain and behavior. *eLife*, *7*, e32962. https://doi.org/10.7554/eLife.32962

Hehman, E., Sutherland, C. A. M., Flake, J. K., & Slepian, M. L. (2017). The unique contributions of perceiver and target characteristics in person perception. *Journal of Personality and Social Psychology*, *113*(4), 513–529. https://doi.org/10.1037/pspa0000090

Hehman, E., Xie, S., Ofosu, E., & Nespoli, G. (2018). *Assessing the point at which averages are stable: A tool illustrated in the context of person perception*. OSF. https://doi.org/10.31234/osf.io/2n6jq

Hu, Y., Parde, C. J., Hill, M. Q., Mahmood, N., & O'Toole, A. J. (2018). First impressions of personality traits from body shapes. *Psychological Science*, *29*(12), 1969–1983. https://doi.org/10.1177/0956797618799300

Illithova, B., Young, A. W., Chu, M., & Sutherland, C. A. M. (2025). Conceptual trait associations predict impressions of highly variable faces. *British Journal of Psychology*, *117*(1), 337–355. https://doi.org/10.1111/bjop.70031

Imhoff, R., Woelki, J., Hanke, S., & Dotsch, R. (2013). Warmth and competence in your face! Visual encoding of stereotype content. *Frontiers in Psychology*, *4*, 386. https://doi.org/10.3389/fpsyg.2013.00386

Irvine, M., & Lavan, N. (2026). Can conceptual beliefs shape impressions from voices? *Psychonomic Bulletin & Review*, *33*(4), 125. https://doi.org/10.3758/s13423-026-02876-w

Jain, P., & Schiller, D. (2026). From first impressions to bonds: The neural dynamics of social relationships. *Neuron*, *0*(0). https://doi.org/10.1016/j.neuron.2026.05.031

Judd, C. M., James-Hawkins, L., Yzerbyt, V., & Kashima, Y. (2005). Fundamental dimensions of social judgment: Understanding the relations between judgments of competence and

warmth. *Journal of Personality and Social Psychology*, *89*(6), 899–913. https://doi.org/10.1037/0022-3514.89.6.899

Judd, C. M., Westfall, J., & Kenny, D. A. (2012). Treating stimuli as a random factor in social psychology: A new and comprehensive solution to a pervasive but largely ignored problem. *Journal of Personality and Social Psychology*, *103*(1), 54–69. https://doi.org/10.1037/a0028347

Koch, A., Imhoff, R., Dotsch, R., Unkelbach, C., & Alves, H. (2016). The ABC of stereotypes about groups: Agency/socioeconomic success, conservative–progressive beliefs, and communion. *Journal of Personality and Social Psychology*, *110*(5), 675–709. https://doi.org/10.1037/pspa0000046

Kramer, R. S. S., & Jones, A. L. (2020). Sequential effects in facial attractiveness judgments using cross-classified models: Investigating perceptual and response biases. *Journal of Experimental Psychology: Human Perception and Performance*, *46*(12), 1476–1489. https://doi.org/10.1037/xhp0000869

Kramer, R. S. S., Young, A. W., & Burton, A. M. (2018). Understanding face familiarity. *Cognition*, *172*, 46–58. https://doi.org/10.1016/j.cognition.2017.12.005

Kriegeskorte, N. (2008). Representational similarity analysis – connecting the branches of systems neuroscience. *Frontiers in Systems Neuroscience*. https://doi.org/10.3389/neuro.06.004.2008

Kunda, Z., & Thagard, P. (1996). Forming impressions from stereotypes, traits, and behaviors: A parallel-constraint-satisfaction theory. *Psychological Review*, *103*(2), 284–308. https://doi.org/10.1037/0033-295X.103.2.284

Lavan, N., Rinke, P., & Scharinger, M. (2024). The time course of person perception from voices

in the brain. *Proceedings of the National Academy of Sciences of the United States of America*, *121*(26), e2318361121. https://doi.org/10.1073/pnas.2318361121

Lee, S., Ying, J., Dey, A., Jeon, Y.-N., & Issa, E. B. (2026). *Efficient task generalization and humanlike face perception in models that learn to discriminate face geometry* (p. 2026.01.31.703048). bioRxiv. https://doi.org/10.64898/2026.01.31.703048

Lin, C., Keles, U., & Adolphs, R. (2021). Four dimensions characterize attributions from faces using a representative set of English trait words. *Nature Communications*, *12*(1), Article 1. https://doi.org/10.1038/s41467-021-25500-y

Lin, C., & Thornton, M. A. (2024). *Bottom-up and top-down information determinants of naturalistic trait impression updating*. https://doi.org/10.31234/osf.io/jxzca

Liu, Z., Luo, P., Wang, X., & Tang, X. (2015). Deep Learning Face Attributes in the Wild. *2015 IEEE International Conference on Computer Vision (ICCV)*, 3730–3738. https://doi.org/10.1109/ICCV.2015.425

Lu, J., & Lin, C. (2025). Network models reveal high-dimensional social inferences in naturalistic settings beyond latent construct models. *Communications Psychology*, *3*, 98. https://doi.org/10.1038/s44271-025-00275-w

Matuschek, H., Kliegl, R., Vasishth, S., Baayen, H., & Bates, D. (2017). Balancing Type I error and power in linear mixed models. *Journal of Memory and Language*, *94*, 305–315. https://doi.org/10.1016/j.jml.2017.01.001

Mileva, V. R., Cowan, M. L., Cobey, K. D., Knowles, K. K., & Little, A. C. (2014). In the face of dominance: Self-perceived and other-perceived dominance are positively associated with facial-width-to-height ratio in men. *Personality and Individual Differences*, *69*, 115–118. https://doi.org/10.1016/j.paid.2014.05.019

Nicolas, G., Bai, X., & Fiske, S. T. (2022). A spontaneous stereotype content model: Taxonomy, properties, and prediction. *Journal of Personality and Social Psychology*, *123*(6), 1243–1263. https://doi.org/10.1037/pspa0000312

Oh, D., Dotsch, R., Porter, J., & Todorov, A. (2020). Gender biases in impressions from faces: Empirical studies and computational models. *Journal of Experimental Psychology: General*, *149*(2), 323–342. https://doi.org/10.1037/xge0000638

Oh, D., Dotsch, R., & Todorov, A. (2019). Contributions of shape and reflectance information to social judgments from faces. *Vision Research*, *165*, 131–142. https://doi.org/10.1016/j.visres.2019.10.010

Oh, D., Martin, J. D., & Freeman, J. B. (2022). Personality Across World Regions Predicts Variability in the Structure of Face Impressions. *Psychological Science*, *33*(8), 1240–1256. https://doi.org/10.1177/09567976211072814

Oh, D., Walker, M., & Freeman, J. B. (2021). Person knowledge shapes face identity perception. *Cognition*, *217*, 104889. https://doi.org/10.1016/j.cognition.2021.104889

Oldmeadow, J. A., Sutherland, C. A. M., & Young, A. W. (2013). Facial Stereotype Visualization Through Image Averaging. *Social Psychological and Personality Science*, *4*(5), 615–623. https://doi.org/10.1177/1948550612469820

Olivola, C. Y., Funk, F., & Todorov, A. (2014). Social attributions from faces bias human choices. *Trends in Cognitive Sciences*, *18*(11), 566–570. https://doi.org/10.1016/j.tics.2014.09.007

Oosterhof, N. N., & Todorov, A. (2008). The functional basis of face evaluation. *Proceedings of the National Academy of Sciences*, *105*(32), 11087–11092. https://doi.org/10.1073/pnas.0805664105

Parde, C. J., Hu, Y., Castillo, C., Sankaranarayanan, S., & O'Toole, A. J. (2019). Social Trait Information in Deep Convolutional Neural Networks Trained for Face Identification. *Cognitive Science*, *43*(6), e12729. https://doi.org/10.1111/cogs.12729

Peterson, J. C., Uddenberg, S., Griffiths, T. L., Todorov, A., & Suchow, J. W. (2022). Deep models of superficial face judgments. *Proceedings of the National Academy of Sciences*, *119*(17), e2115228119. https://doi.org/10.1073/pnas.2115228119

Popal, H., Wang, Y., & Olson, I. R. (2019). A Guide to Representational Similarity Analysis for Social Neuroscience. *Social Cognitive and Affective Neuroscience*, *14*(11), 1243–1253. https://doi.org/10.1093/scan/nsz099

Ramesh, D. S., Heijnen, S., Hekster, O., Spreeuwers, L., & de Wit, F. (2022). Facial recognition as a tool to identify Roman emperors: Towards a new methodology. *Humanities and Social Sciences Communications*, *9*(1), 78. https://doi.org/10.1057/s41599-022-01090-y

Ramon, M., & Gobbini, M. I. (2018). Familiarity matters: A review on prioritized processing of personally familiar faces. *Visual Cognition*, *26*(3), 179–195. https://doi.org/10.1080/13506285.2017.1405134

Ray-Mukherjee, J., Nimon, K., Mukherjee, S., Morris, D. W., Slotow, R., & Hamer, M. (2014). Using commonality analysis in multiple regressions: A tool to decompose regression effects in the face of multicollinearity. *Methods in Ecology and Evolution*, *5*(4), 320–328. https://doi.org/10.1111/2041-210X.12166

Ritchie, K. L., Palermo, R., & Rhodes, G. (2017). Forming impressions of facial attractiveness is mandatory. *Scientific Reports*, *7*(1), 469. https://doi.org/10.1038/s41598-017-00526-9

Said, C. P., Sebe, N., & Todorov, A. (2009). Structural resemblance to emotional expressions predicts evaluation of emotionally neutral faces. *Emotion*, *9*(2), 260–264.

https://doi.org/10.1037/a0014681

Shen, X., Mann, T. C., & Ferguson, M. J. (2020). Beware a dishonest face?: Updating face-based implicit impressions using diagnostic behavioral information. *Journal of Experimental Social Psychology*, *86*, 103888. https://doi.org/10.1016/j.jesp.2019.103888

Stolier, R. M., Hehman, E., & Freeman, J. B. (2020). Trait knowledge forms a common structure across social cognition. *Nature Human Behaviour*, *4*(4), 361–371. https://doi.org/10.1038/s41562-019-0800-6

Stolier, R. M., Hehman, E., Keller, M. D., Walker, M., & Freeman, J. B. (2018). The conceptual structure of face impressions. *Proceedings of the National Academy of Sciences of the United States of America*, *115*(37), 9210–9215. https://doi.org/10.1073/pnas.1807222115

Sutherland, C. A. M., Burton, N. S., Wilmer, J. B., Blokland, G. A. M., Germine, L., Palermo, R., Collova, J. R., & Rhodes, G. (2020). Individual differences in trust evaluations are shaped mostly by environments, not genes. *Proceedings of the National Academy of Sciences*, *117*(19), 10218–10224. https://doi.org/10.1073/pnas.1920131117

Sutherland, C. A. M., Oldmeadow, J. A., Santos, I. M., Towler, J., Michael Burt, D., & Young, A. W. (2013). Social inferences from faces: Ambient images generate a three-dimensional model. *Cognition*, *127*(1), 105–118. https://doi.org/10.1016/j.cognition.2012.12.001

Tea-makorn, P. P., & Kosinski, M. (2020). Spouses' faces are similar but do not become more similar with time. *Scientific Reports*, *10*(1), 17001. https://doi.org/10.1038/s41598-020-73971-8

Thornton, M. A., & Mitchell, J. P. (2017). Consistent Neural Activity Patterns Represent Personally Familiar People. *Journal of Cognitive Neuroscience*, *29*(9), 1583–1594.

https://doi.org/10.1162/jocn_a_01151

Todorov, A. (2008). Evaluating Faces on Trustworthiness: Extension of Systems for Recognition of Emotions Signaling Approach/Avoidance Behaviors. *Annals of the New York Academy of Sciences*, *1124*(1), 208–224. https://doi.org/10.1196/annals.1440.012

Todorov, A., Gobbini, M. I., Evans, K. K., & Haxby, J. V. (2007). Spontaneous retrieval of affective person knowledge in face perception. *Neuropsychologia*, *45*(1), 163–173. https://doi.org/10.1016/j.neuropsychologia.2006.04.018

Todorov, A., Mandisodza, A. N., Goren, A., & Hall, C. C. (2005). Inferences of Competence from Faces Predict Election Outcomes. *Science*, *308*(5728), 1623–1626. https://doi.org/10.1126/science.1110589

Todorov, A., Olivola, C. Y., Dotsch, R., & Mende-Siedlecki, P. (2015). Social Attributions from Faces: Determinants, Consequences, Accuracy, and Functional Significance. *Annual Review of Psychology*, *66*(1), 519–545. https://doi.org/10.1146/annurev-psych-113011-143831

Toscano, H., Schubert, T. W., & Sell, A. N. (2014). Judgments of Dominance from the Face Track Physical Strength. *Evolutionary Psychology*, *12*(1), 1–18. https://doi.org/10.1177/147470491401200101

Vernon, R. J. W., Sutherland, C. A. M., Young, A. W., & Hartley, T. (2014). Modeling first impressions from highly variable facial images. *Proceedings of the National Academy of Sciences of the United States of America*, *111*(32), E3353-3361. https://doi.org/10.1073/pnas.1409860111

Willis, J., & Todorov, A. (2006). First Impressions: Making Up Your Mind After a 100-Ms Exposure to a Face. *Psychological Science*, *17*(7), 592–598.

https://doi.org/10.1111/j.1467-9280.2006.01750.x

Wilson, J. P., & Rule, N. O. (2015). Facial trustworthiness predicts extreme criminal-sentencing outcomes. *Psychological Science*, *26*(8), 1325–1331. https://doi.org/10.1177/0956797615590992

Xie, S. Y., Flake, J. K., Stolier, R. M., Freeman, J. B., & Hehman, E. (2021). Facial Impressions Are Predicted by the Structure of Group Stereotypes. *Psychological Science*, *32*(12), 1979–1993. https://doi.org/10.1177/09567976211024259

Young, A. W., & Burton, A. M. (2018). Are We Face Experts? *Trends in Cognitive Sciences*, *22*(2), 100–110. https://doi.org/10.1016/j.tics.2017.11.007

Yu, H., Cao, R., Lin, C., & Wang, S. (2022). Distinct neurocognitive bases for social trait judgments of faces in autism spectrum disorder. *Translational Psychiatry*, *12*(1), Article 1. https://doi.org/10.1038/s41398-022-01870-9

Zebrowitz, L. A., & McDonald, S. M. (1991). The impact of litigants' baby-facedness and attractiveness on adjudications in small claims courts. *Law and Human Behavior*, *15*(6), 603–623. https://doi.org/10.1007/BF01065855

Zhao, S., Cao, R., Lin, C., Wang, S., & Yu, H. (2024). Differences in the link between social trait judgment and socio-emotional experience in neurotypical and autistic individuals. *Scientific Reports*, *14*(1), Article 1. https://doi.org/10.1038/s41598-024-56005-5

Supplementary Materials for

A dual-route model of facial trait impressions: Dissociating the perceptual and conceptual contributions

S1. Representational similarity analysis: full results

Table S1

Spearman Correlations Between Each Trait Representational Space and the Semantic and Visual Representational Spaces

U.S. sample

Outcome	ρ_{sem}	p_{perm}	p_{maxt}	ρ_{vis}	p_{perm}	p_{maxt}	$\Delta\rho$	95% CI	p_{boot}
Trait space	.36	< .001	—	.32	< .001	—	.04	[−.18, .27]	.679
Warm	.08	.121	.696	.06	.138	.677	.03	[−.15, .20]	.763
Critical	−.08	.194	.759	.00	.981	1.000	−.08	[−.23, .08]	.305
Competent	.11	.108	.387	.02	.698	1.000	.09	[−.08, .27]	.326
Practical	.08	.167	.685	.09	.017	.118	−.01	[−.17, .15]	.898
Feminine	.34	< .001	< .001	.24	< .001	< .001	.10	[−.11, .31]	.336
Strong	.18	.007	.028	.19	< .001	< .001	−.01	[−.20, .17]	.940
Youthful	.06	.291	.881	.16	< .001	.001	−.10	[−.23, .05]	.190
Charismatic	.05	.431	.967	.06	.124	.568	−.01	[−.18, .17]	.886

Chinese sample

Outcome	ρ_{sem}	p_{perm}	p_{maxt}	ρ_{vis}	p_{perm}	p_{maxt}	$\Delta\rho$	95% CI	p_{boot}
Trait space	.39	< .001	—	.69	< .001	—	−.30	[−.45, −.13]	< .001
Warm	−.09	.091	.464	−.04	.257	.897	−.05	[−.17, .09]	.510
Critical	.19	.003	.012	.11	.007	.046	.08	[−.10, .27]	.397
Competent	.12	.012	.142	.17	< .001	.002	−.05	[−.21, .10]	.496
Practical	.21	< .001	.005	.27	< .001	< .001	−.06	[−.27, .14]	.614
Feminine	.24	< .001	.002	.62	< .001	< .001	−.38	[−.51, −.22]	< .001
Strong	.17	.003	.020	.36	< .001	< .001	−.19	[−.36, −.02]	.029
Youthful	.39	< .001	< .001	.36	< .001	< .001	.03	[−.14, .18]	.732
Charismatic	.09	.090	.397	.11	.004	.030	−.02	[−.17, .14]	.798
Trustworthy	.01	.906	1.000	.03	.339	.967	−.03	[−.15, .11]	.641
Attractive	.27	< .001	< .001	.35	< .001	< .001	−.08	[−.28, .12]	.409

Note. ρ_{sem} and ρ_{vis} are Spearman correlations between the behavioural trait RDM and the semantic and visual model RDMs. p_{perm} is the uncorrected permutation p (5,000 permutations of the target labels). p_{maxt} is the max-T family-wise corrected p (5,000 permutations; family = all traits within a channel within a sample); the trait space is a single outcome per sample and therefore carries no family, shown as —. $\Delta\rho$ is the semantic-minus-visual difference with its 95% percentile interval from a bootstrap over the 50 targets (5,000 resamples) and its two-sided p_{boot}; positive values favour the semantic route.

S2. Variance partitioning: full results

Table S2

Variance in Each Trait Representational Space Uniquely Attributable to the Semantic and Visual Routes

U.S. sample

Outcome	Unique sem (%)	95% CI	p_{perm}	p_{maxt}	Unique vis (%)	95% CI	p_{perm}	p_{maxt}	Shared (%)	Total R^2 (%)	$\Delta\Delta R^2$ (%)	p_{boot}
Trait space	8.7	[2.7, 18.7]	< .001	—	8.7	[2.5, 18.5]	< .001	—	3.9	21.3	0.1	.934
Warm	0.6	[0.0, 5.5]	.202	.874	0.5	[0.0, 3.8]	.085	.530	0.2	1.3	0.1	.900
Critical	0.9	[0.0, 5.6]	.157	.678	0.2	[0.0, 2.3]	.316	.917	-0.1	1.0	0.7	.523
Competent	1.9	[0.0, 9.1]	.076	.264	0.0	[0.0, 1.6]	.992	1.000	0.1	1.9	1.9	.299
Practical	0.7	[0.0, 5.0]	.245	.825	0.6	[0.0, 3.9]	.055	.325	0.3	1.6	0.0	.934
Feminine	9.2	[3.1, 18.9]	< .001	< .001	5.0	[0.8, 12.1]	< .001	< .001	3.0	17.3	4.2	.436

Strong	2.7	[0.0, 10.2]	.019	.106	2.7	[0.2, 8.3]	< .001	< .001	1.2	6.6	-0.0	.995
Youthful	0.1	[0.0, 2.8]	.629	1.000	3.3	[0.4, 9.3]	< .001	< .001	0.3	3.7	-3.2	.131
Charismatic	0.2	[0.0, 4.4]	.548	.993	0.2	[0.0, 2.8]	.296	.873	0.1	0.5	-0.0	.852

Chinese sample

Outcome	Unique sem (%)	95% CI	p_{perm}	p_{maxt}	Unique vis (%)	95% CI	p_{perm}	p_{maxt}	Shared (%)	Total R^2 (%)	$\Delta\Delta R^2$ (%)	p_{boot}
Trait space	2.5	[0.2, 7.4]	< .001	—	34.9	[24.1, 46.0]	< .001	—	14.3	51.7	-32.3	< .001
Warm	0.7	[0.0, 3.6]	.178	.749	0.0	[0.0, 1.6]	.945	1.000	0.1	0.9	0.7	.442
Critical	2.7	[0.0, 11.2]	.017	.068	0.0	[0.0, 3.3]	.734	1.000	0.7	3.4	2.7	.346
Competent	0.7	[0.0, 5.5]	.142	.789	2.4	[0.1, 8.3]	< .001	.005	1.6	4.6	-1.7	.529

Practical	1.8	[0.0, 10.0]	.008	.224	4.4	[0.5, 13.0]	< .001	< .001	3.5	9.7	-2.6	.602
Feminine	0.0	[0.0, 2.1]	.672	1.000	29.4	[18.4, 41.2]	< .001	< .001	5.3	34.7	-29.4	< .001
Strong	0.8	[0.0, 4.9]	.184	.699	10.1	[2.8, 21.4]	< .001	< .001	4.3	15.2	-9.3	.039
Youthful	8.3	[2.4, 16.4]	< .001	< .001	6.2	[1.1, 15.1]	< .001	< .001	8.6	23.1	2.1	.710
Charismatic	0.6	[0.0, 4.6]	.234	.808	0.9	[0.0, 5.7]	.033	.185	0.9	2.4	-0.3	.915
Trustworthy	0.0	[0.0, 2.5]	.816	1.000	0.1	[0.0, 1.9]	.505	.998	0.0	0.1	-0.1	.915
Attractive	2.8	[0.1, 10.0]	.009	.061	8.2	[1.8, 18.4]	< .001	< .001	6.0	17.0	-5.4	.354

Note. Values are percentages of variance in the trait RDM, from ordinary least squares on the raw pairwise dissimilarities. Unique variance is the drop in explained variance when that route is removed from the full model. p_{perm} is the identity-level permutation test (5,000 permutations of the target labels) and p_{maxt} its max-T correction within channel and sample; the trait space carries no family, shown as —. Confidence intervals are percentile intervals from a

bootstrap over the 50 targets (5,000 resamples). $\Delta\Delta R^2$ is the semantic-minus-visual difference in unique variance, computed on the same resamples so that the two routes are paired.

S3. Familiarity moderation: full linear mixed model results

Table S3

Familiarity Moderation of the Semantic and Visual Contributions to Trait Representation

Panel A. U.S. sample

Outcome	Level	*N* obs	β Sem×Fam	95% CI	*p*	p_{Holm}	β Vis×Fam	95% CI	*p*	p_{Holm}
Trait space	L0	489,741	.005	[−.011, .020]	.563	—	−.001	[−.016, .013]	.854	—
Warm	L0	464,055	−.003	[−.013, .008]	.639	1.000	−.006	[−.013, .001]	.109	.437
Critical	L1	447,155	−.001	[−.006, .005]	.818	1.000	−.003	[−.007, .000]	.080	.401
Competent	L1	454,525	−.000	[−.006, .006]	.970	1.000	−.005	[−.009, −.001]	.014	.097
Practical	L0	448,175	.003	[−.003, .008]	.372	1.000	−.007	[−.012, −.002]	.003	.026
Feminine	L0	433,689	.009	[−.016, .035]	.466	1.000	.004	[−.025, .032]	.796	1.000

Strong	L0	465,295	.020	[.007, .033]	.002	.016	−.004	[−.016, .007]	.451	1.000
Youthful	L0	460,530	−.008	[−.024, .009]	.346	1.000	.005	[−.008, .017]	.473	1.000
Charismatic	L0	461,680	−.000	[−.008, .008]	.969	1.000	−.005	[−.011, .000]	.055	.329

Panel B. Chinese sample

Outcome	Level	*N* obs	β Sem×Fam	95% CI	*p*	p_{Holm}	β Vis×Fam	95% CI	*p*	p_{Holm}
Trait space	L0	389,137	.023	[.006, .039]	.007	—	.012	[−.001, .025]	.073	—
Warm	L1	381,067	−.005	[−.015, .004]	.250	.749	.004	[−.002, .011]	.156	1.000
Critical	L2	379,789	.007	[−.001, .014]	.102	.408	−.003	[−.009, .003]	.285	1.000
Competent	L0	374,705	.035	[.021, .050]	< .001	< .001	−.005	[−.016, .006]	.368	1.000
Practical	L1	378,854	.037	[.028, .046]	< .001	< .001	−.004	[−.011, .004]	.346	1.000
Feminine	L0	373,388	.016	[−.017, .049]	.350	.749	.019	[−.006, .043]	.141	1.000

Strong	L0	383,109	.017	[−.000, .034]	.052	.286	−.002	[−.019, .014]	.796	1.000
Youthful	L0	384,275	.021	[.000, .042]	.048	.286	−.000	[−.015, .014]	.969	1.000
Charismatic	L0	378,918	−.018	[−.032, −.004]	.012	.081	.004	[−.006, .014]	.445	1.000
Trustworthy	L0	381,025	.016	[.004, .027]	.008	.067	−.002	[−.011, .007]	.626	1.000
Attractive	L0	381,419	−.004	[−.018, .009]	.531	.749	−.002	[−.016, .013]	.803	1.000

Note. Interaction coefficients from linear mixed models predicting pairwise trait distance from semantic distance, visual distance, pair-mean familiarity, the two focal interactions, and absolute within-pair familiarity difference. Coefficients are fully standardized: predictors *z*-scored and the fitted coefficient divided by the *SD* of the outcome, so β is in *SD* units of trait distance and is comparable across outcomes and samples. Positive β: the route contributes more for better-known pairs. *Level* is the random-effects structure retained for that outcome (see Table S4). p_{Holm} is Holm-Bonferroni corrected within sample and channel; the trait space is a single outcome and is not part of any family, shown as —.

S4. Random-effects reduction ladder: fit statistics for model selection

Table S4

Fit Statistics at Every Level of the Pre-Specified Random-Effects Reduction Ladder, With the Retained Model in Bold

Panel A. U.S. sample

Outcome	Level	*k*	log *L*	AIC	Converged
Trait space	**L0**	**63**	**-993,086**	**1,986,315**	**Yes**
Trait space	L1	41	-993,459	1,987,015	Yes
Trait space	L2	33	—	—	No
Trait space	L3	23	—	—	No
Trait space	L4	12	-1,008,868	2,017,777	Yes
Trait space	L5	8	-1,010,290	2,020,613	Yes
Trait space	L6	3	-1,012,756	2,025,534	Yes
Warm	**L0**	**63**	**-818,235**	**1,636,613**	**Yes**
Warm	L1	41	-818,335	1,636,768	Yes
Warm	L2	33	—	—	No
Warm	L3	23	—	—	No
Warm	L4	12	-820,390	1,640,820	Yes
Warm	L5	8	-821,970	1,643,972	Yes

Warm	L6	3	-823,091	1,646,203	Yes
Critical	L0	63	—	—	No
Critical	**L1**	**41**	**-828,350**	**1,656,798**	**Yes**
Critical	L2	33	—	—	No
Critical	L3	23	—	—	No
Critical	L4	12	-828,811	1,657,663	Yes
Critical	L5	8	-829,618	1,659,267	Yes
Critical	L6	3	-830,047	1,660,116	Yes
Competent	L0	63	—	—	No
Competent	**L1**	**41**	**-751,582**	**1,503,262**	**Yes**
Competent	L2	33	—	—	No
Competent	L3	23	—	—	No
Competent	L4	12	-752,179	1,504,397	Yes
Competent	L5	8	-755,232	1,510,495	Yes
Competent	L6	3	-755,921	1,511,865	Yes
Practical	**L0**	**63**	**-792,863**	**1,585,869**	**Yes**
Practical	L1	41	-792,873	1,585,845	Yes
Practical	L2	33	—	—	No
Practical	L3	23	—	—	No
Practical	L4	12	-793,258	1,586,555	Yes

Practical	L5	8	-794,192	1,588,415	Yes
Practical	L6	3	-794,880	1,589,782	Yes
Feminine	**L0**	**63**	**-867,337**	**1,734,815**	**Yes**
Feminine	L1	41	-868,716	1,737,529	Yes
Feminine	L2	33	-869,700	1,739,481	Yes
Feminine	L3	23	-909,822	1,819,706	Yes
Feminine	L4	12	-909,987	1,820,014	Yes
Feminine	L5	8	-910,086	1,820,204	Yes
Feminine	L6	3	-913,026	1,826,075	Yes
Strong	**L0**	**63**	**-818,179**	**1,636,499**	**Yes**
Strong	L1	41	-818,368	1,636,833	Yes
Strong	L2	33	-819,050	1,638,182	Yes
Strong	L3	23	—	—	No
Strong	L4	12	-822,820	1,645,680	Yes
Strong	L5	8	-824,394	1,648,821	Yes
Strong	L6	3	-826,204	1,652,429	Yes
Youthful	**L0**	**63**	**-810,974**	**1,622,091**	**Yes**
Youthful	L1	41	-811,420	1,622,938	Yes
Youthful	L2	33	—	—	No
Youthful	L3	23	-824,557	1,649,175	Yes

Youthful	L4	12	-824,673	1,649,385	Yes
Youthful	L5	8	-825,392	1,650,817	Yes
Youthful	L6	3	-826,033	1,652,089	Yes
Charismatic	**L0**	**63**	**-830,401**	**1,660,945**	**Yes**
Charismatic	L1	41	—	—	No
Charismatic	L2	33	—	—	No
Charismatic	L3	23	—	—	No
Charismatic	L4	12	-831,136	1,662,313	Yes
Charismatic	L5	8	-832,449	1,664,930	Yes
Charismatic	L6	3	-833,084	1,666,191	Yes

Panel B. Chinese sample

Outcome	Level	*k*	log *L*	AIC	Converged
Trait space	**L0**	**63**	**-766,944**	**1,534,031**	**Yes**
Trait space	L1	41	-767,355	1,534,808	Yes
Trait space	L2	33	-768,863	1,537,808	Yes
Trait space	L3	23	-780,074	1,560,209	Yes
Trait space	L4	12	-780,906	1,561,853	Yes
Trait space	L5	8	-783,299	1,566,630	Yes
Trait space	L6	3	-787,053	1,574,127	Yes

Warm	L0	63	—	—	No
Warm	**L1**	**41**	**-633,639**	**1,267,377**	**Yes**
Warm	L2	33	-634,179	1,268,440	Yes
Warm	L3	23	-634,388	1,268,838	Yes
Warm	L4	12	-634,809	1,269,657	Yes
Warm	L5	8	-636,717	1,273,466	Yes
Warm	L6	3	-637,811	1,275,644	Yes
Critical	L0	63	—	—	No
Critical	L1	41	—	—	No
Critical	**L2**	**33**	**-658,438**	**1,316,957**	**Yes**
Critical	L3	23	—	—	No
Critical	L4	12	-660,027	1,320,094	Yes
Critical	L5	8	-661,425	1,322,883	Yes
Critical	L6	3	-663,603	1,327,227	Yes
Competent	**L0**	**63**	**-574,392**	**1,148,925**	**Yes**
Competent	L1	41	-574,550	1,149,198	Yes
Competent	L2	33	-576,384	1,152,850	Yes
Competent	L3	23	-578,138	1,156,337	Yes
Competent	L4	12	-578,963	1,157,966	Yes
Competent	L5	8	-583,016	1,166,064	Yes

Competent	L6	3	-585,373	1,170,768	Yes
Practical	L0	63	—	—	No
Practical	**L1**	**41**	**-604,114**	**1,208,325**	**Yes**
Practical	L2	33	-605,305	1,210,692	Yes
Practical	L3	23	-607,331	1,214,723	Yes
Practical	L4	12	-607,899	1,215,837	Yes
Practical	L5	8	-610,530	1,221,091	Yes
Practical	L6	3	-613,717	1,227,455	Yes
Feminine	**L0**	**63**	**-703,988**	**1,408,119**	**Yes**
Feminine	L1	41	-705,934	1,411,966	Yes
Feminine	L2	33	-706,902	1,413,886	Yes
Feminine	L3	23	-750,775	1,501,611	Yes
Feminine	L4	12	-751,508	1,503,055	Yes
Feminine	L5	8	-751,580	1,503,193	Yes
Feminine	L6	3	-754,326	1,508,675	Yes
Strong	**L0**	**63**	**-610,941**	**1,222,024**	**Yes**
Strong	L1	41	-611,399	1,222,896	Yes
Strong	L2	33	-611,999	1,224,080	Yes
Strong	L3	23	-619,747	1,239,555	Yes
Strong	L4	12	-620,393	1,240,826	Yes

Strong	L5	8	-621,783	1,243,598	Yes
Strong	L6	3	-626,367	1,252,757	Yes
Youthful	**L0**	**63**	**-607,579**	**1,215,301**	**Yes**
Youthful	L1	41	—	—	No
Youthful	L2	33	-608,426	1,216,934	Yes
Youthful	L3	23	-637,927	1,275,915	Yes
Youthful	L4	12	-638,942	1,277,924	Yes
Youthful	L5	8	-639,540	1,279,113	Yes
Youthful	L6	3	-642,271	1,284,563	Yes
Charismatic	**L0**	**63**	**-630,491**	**1,261,125**	**Yes**
Charismatic	L1	41	-630,678	1,261,454	Yes
Charismatic	L2	33	-631,893	1,263,868	Yes
Charismatic	L3	23	-633,295	1,266,652	Yes
Charismatic	L4	12	-634,088	1,268,217	Yes
Charismatic	L5	8	-637,051	1,274,134	Yes
Charismatic	L6	3	-640,249	1,280,520	Yes
Trustworthy	**L0**	**63**	**-612,995**	**1,226,132**	**Yes**
Trustworthy	L1	41	-613,049	1,226,195	Yes
Trustworthy	L2	33	-614,048	1,228,178	Yes
Trustworthy	L3	23	-614,536	1,229,133	Yes

Trustworthy	L4	12	-615,142	1,230,324	Yes
Trustworthy	L5	8	-617,829	1,235,691	Yes
Trustworthy	L6	3	-619,773	1,239,568	Yes
Attractive	**L0**	**63**	**-646,255**	**1,292,651**	**Yes**
Attractive	L1	41	-646,463	1,293,024	Yes
Attractive	L2	33	-647,613	1,295,308	Yes
Attractive	L3	23	-654,943	1,309,949	Yes
Attractive	L4	12	-656,115	1,312,271	Yes
Attractive	L5	8	-658,093	1,316,219	Yes
Attractive	L6	3	-663,555	1,327,132	Yes

Note. The retained model, in bold, is the highest level returning a usable non-singular fit; selection was on identifiability, not on fit. *k* is the number of covariance parameters, from L0 (all five varying terms at participant and at each target identity) down to L6 (random intercepts only). Target-level terms are stripped before participant-level terms, so the participant-level slopes for both focal interactions are present in all 20 retained models. Rejected maximal fits can attain a higher likelihood and lower AIC than the model retained; a near-singular Hessian means the nominal parameter count overstates the number of identified parameters, so those comparisons are not informative. *Converged* = No covers failure to converge, a singular fit, and convergence accompanied by a warning, which the fitting script does not distinguish. AIC is not reproducible from *k* alone: it is $2K - 2 \log L$ with *K* the count of all estimated parameters, which is *k* plus the seven fixed effects and the residual *SD*, so $K = k + 8$ here ($k + 7$ in Table S6, where the models carry no familiarity-difference term). The five rejected maximal fits were refitted independently

with explicit diagnostics, which confirmed that the maximal structure is not identifiable from those data.

S5. Collinearity between the semantic and visual RDMs

Table S5.1

Correlation Between the Semantic and Visual Model Representational Spaces

Sample	Split	*n* targets	*n* pairs	ρ	r	Shared variance (%)	VIF
U.S.	All targets	50	1,225	.17	.18	3.3	1.03
U.S.	More familiar	25	300	.21	.23	5.2	1.05
U.S.	Less familiar	25	300	.18	.17	3.0	1.03
China	All targets	50	1,225	.34	.37	14.0	1.16
China	More familiar	26	325	.37	.41	16.7	1.20
China	Less familiar	24	276	.39	.38	14.6	1.17

Note. ρ is the Spearman correlation between the two flattened RDMs, the descriptive used for the RSA. r is the Pearson correlation, which governs the variance partitioning: that analysis is ordinary least squares on the raw dissimilarities, so the shared variance is r^2 and the variance inflation is $1/(1 - r^2)$. Both are reported so that neither analysis is described by the wrong coefficient.

Table S5.2

Variance Inflation Factors for the Fixed Effects of the Perceiver-Level Mixed Models

Sample	Term	VIF	R^2 on other predictors
U.S.	Semantic distance	1.05	.047
U.S.	Visual distance	1.03	.033
U.S.	Pair-mean familiarity	1.44	.307
U.S.	Semantic × Familiarity	1.07	.069
U.S.	Visual × Familiarity	1.04	.036
U.S.	Familiarity difference	1.41	.293
China	Semantic distance	1.20	.163
China	Visual distance	1.17	.143
China	Pair-mean familiarity	1.26	.209
China	Semantic × Familiarity	1.17	.142
China	Visual × Familiarity	1.17	.142
China	Familiarity difference	1.26	.207

Note. Computed on the trait-space model; the predictor matrix is identical across outcomes, so these values apply to every per-trait model as well. All values fall far below any conventional threshold, the strictest in general use being 4. The two focal interaction terms are among the least inflated predictors, so the moderation estimates are not destabilised by overlap between the routes; they are not inflated by their product construction because the constituent variables were *z*-scored before the product was formed. In the U.S. models the familiarity difference is a deterministic function of pair-mean familiarity, since with a binary recognition

item the difference is non-zero exactly when one target of the two is recognised, so the values near 1.4 reflect a three-level moderator entered saturated rather than genuine collinearity.

S6. Binarised moderator: sensitivity analysis

Table S6

Familiarity Moderation With the Moderator Binarised Directly

Panel A. U.S. sample

Outcome	Level	*N* obs	*β* Sem×Fam	95% CI	*p*	p_{Holm}	*β* Vis×Fam	95% CI	*p*	p_{Holm}
Trait space	L0	310,288	.025	[−.013, .063]	.201	—	.005	[−.027, .038]	.746	—
Warm	L1	293,980	.000	[−.021, .021]	.981	1.000	−.003	[−.017, .012]	.726	1.000
Critical	L0	283,961	.004	[−.020, .027]	.755	1.000	−.003	[−.019, .012]	.689	1.000
Competent	L4	287,128	−.001	[−.012, .010]	.874	1.000	−.019	[−.029, −.009]	< .001	.001
Practical	L4	284,803	.017	[.005, .028]	.005	.030	−.026	[−.037, −.016]	< .001	< .001

Feminine	L1	274,575	.079	[.062, .095]	< .001	< .001	−.026	[−.037, −.015]	< .001	< .001
Strong	L0	295,181	.053	[.018, .088]	.003	.019	−.009	[−.041, .024]	.601	1.000
Youthful	L4	291,292	−.009	[−.020, .002]	.127	.508	−.031	[−.041, −.021]	< .001	< .001
Charismatic	L2	292,349	.015	[−.003, .032]	.095	.477	−.014	[−.027, −.001]	.034	.134

Panel B. Chinese sample

Outcome	Level	*N* obs	β Sem×Fam	95% CI	*p*	p_{Holm}	β Vis×Fam	95% CI	*p*	p_{Holm}
Trait space	L0	266,666	.043	[.000, .085]	.048	—	.002	[−.036, .040]	.920	—
Warm	L1	260,742	−.018	[−.041, .005]	.130	.651	−.010	[−.029, .009]	.285	1.000
Critical	L2	260,428	−.002	[−.025, .021]	.864	.864	−.007	[−.025, .010]	.418	1.000
Competent	L0	256,519	.069	[.025, .112]	.002	.017	−.019	[−.049, .011]	.215	1.000

Practical	L4	259,412	−.035	[−.051, −.019]	< .001	< .001	.043	[.029, .057]	< .001	< .001
Feminine	L0	255,694	.062	[−.023, .148]	.152	.651	.013	[−.045, .072]	.652	1.000
Strong	L1	262,306	.080	[.054, .105]	< .001	< .001	−.040	[−.065, −.015]	.002	.018
Youthful	L0	263,455	.065	[.016, .114]	.010	.060	−.037	[−.076, .001]	.059	.472
Charismatic	L0	259,115	−.028	[−.065, .010]	.152	.651	−.014	[−.046, .018]	.395	1.000
Trustworthy	L1	260,871	.035	[.009, .061]	.008	.055	−.014	[−.036, .007]	.189	1.000
Attractive	L0	260,896	−.022	[−.065, .021]	.325	.651	−.018	[−.053, .016]	.306	1.000

Note. Columns are as in Table S3. Here the moderator is binarised directly rather than entered as the pair mean, and only pairs whose two targets fall on the same side of the split are retained, which discards 34% of the observations. These models also carry no familiarity-difference control, since with a binary item that term is collinear with the moderator by construction (see Table S5.2). The comparison is therefore as much a check on which pairs are analysed as on how the moderator is coded.

The primary outcome replicates: the trait space is positive and significant in China under both codings and null in the U.S. under both. Both U.S. effects that survived correction in the main analysis replicate and strengthen, as does competence in China. Two results do not agree. Practicalness in China reverses sign on the semantic channel, from $\beta = .037$ to $\beta = -.035$, with both codings significant after correction; and the visual route, unmoderated throughout the main analysis in China, gains 2 significant interactions here. The U.S. models gain 2 semantic and 3 visual effects absent under the graded coding. Sign reversals among effects significant under both codings: Semantic × Familiarity China Practical; Visual × Familiarity none. The Chinese practicalness result should therefore be read as conditional on the moderator coding, and competence treated as the better-supported of the two corrected Chinese effects.

S7. Resampling scheme: sensitivity analysis

Every semantic-versus-visual comparison reported in the main text rests on a bootstrap over the 50 targets. This section checks those conclusions against a second target-level scheme with different assumptions.

Table S7

Semantic-Versus-Visual Route Comparison Under Two Target-Level Resampling Schemes

Panel A. U.S. sample

Outcome	$\Delta\rho$	p_{boot}	SE_{jack}	p_{jack}	Agree
Trait space	.04	.679	.113	.707	yes
Warm	.03	.763	.086	.750	yes
Critical	−.08	.305	.077	.312	yes
Competent	.09	.326	.089	.305	yes
Practical	−.01	.898	.078	.897	yes
Feminine	.10	.336	.104	.351	yes
Strong	−.01	.940	.095	.922	yes
Youthful	−.10	.190	.070	.152	yes
Charismatic	−.01	.886	.087	.897	yes

Panel B. Chinese sample

Outcome	$\Delta\rho$	p_{boot}	SE_{jack}	p_{jack}	Agree
Trait space	−.30	< .001	.078	< .001	yes
Warm	−.05	.510	.060	.434	yes
Critical	.08	.397	.096	.386	yes
Competent	−.05	.496	.078	.507	yes
Practical	−.06	.614	.106	.596	yes
Feminine	−.38	< .001	.073	< .001	yes
Strong	−.19	.029	.085	.029	yes
Youthful	.03	.732	.078	.738	yes
Charismatic	−.02	.798	.077	.798	yes
Trustworthy	−.03	.641	.062	.659	yes
Attractive	−.08	.409	.102	.420	yes

Note. $\Delta\rho$ is the semantic-minus-visual difference in Spearman correlation; positive values favour the semantic route. p_{boot} is the two-sided p from a bootstrap over the 50 targets (5,000 resamples), the test used throughout the main text. The jackknife deletes one target at a time and estimates the standard error from the spread of the 50 leave-one-out estimates, giving a Wald p; it is a first-order approximation to the bootstrap, so agreement indicates that a result does not depend on the particular scheme, whereas disagreement would indicate that a single target is carrying the effect. *Agree* records whether the two schemes reach the same verdict at $p < .05$. They agree on 18 of the 18 individual traits and on the trait space in both samples: the two routes separate only for femininity and physical strength in China, and for no outcome in the U.S.

sample. The jackknife standard errors show why. For the U.S. femininity comparison, the one most often cited as a route dissociation, the standard error exceeds the difference itself.

S8.1. Stimulus sets: descriptive statistics

Table S8.1a

Composition of the Two Stimulus Sets

Characteristic	U.S.	China
Targets	50	50
Images per target	10	10
Total images	500	500
Female	17	25
Male	33	25
White	40	—
Black	9	—
Biracial	1	—
Occupation categories	7	7
Most common occupation	Actor/Actress	Actor/Actress/Model

Note. Race was coded for the U.S. stimulus set only, from the CelebA identity annotations used to select those targets; all Chinese targets are Chinese nationals and ethnicity was not coded, so no comparable breakdown is available. Image counts are by design, ten photographs per target, distributed across ten modules so that each module contains one unique image of each target.

Table S8.1b

Occupation Distribution of the Targets in Each Stimulus Set

U.S. occupation	*n*	China occupation	*n*
Actor/Actress	30	Actor/Actress/Model	18
Musician	8	Athlete	9
Athlete	3	Musician	8
Host/Media	3	Entrepreneur	5
Politician/Official	3	Scholar/Writer	5
Actor/Actress/Model	2	Host/Media	4
Director	1	Politician/Official	1

Note. Occupation categories are those used to colour the semantic-space projection in the main text. Counts sum to 50 in each sample.

S8.2. Stimulus sets: individual targets

Table S8.2a

U.S. Target Identities

ID	Name	Gender	Race	Occupation
1	Bre Scullark	Female	Black	Actor/Actress
2	Carey Hart	Male	White	Athlete
3	Zac Efron	Male	White	Actor/Actress
4	Christian Oliver	Male	White	Actor/Actress
5	Conan O'Brien	Male	White	Host/Media
6	Curtis Jackson	Male	Black	Musician
7	Dana Delany	Female	White	Actor/Actress
8	Dean Geyer	Male	Black	Musician
9	Diego Boneta	Male	White	Actor/Actress
10	Dwayne Wade	Male	Black	Athlete
11	Eduardo Noriega	Male	White	Actor/Actress
12	Gabriel Soto	Male	White	Actor/Actress
13	Betty White	Female	White	Actor/Actress
14	George Burns	Male	White	Actor/Actress
15	James Harden	Male	Black	Athlete

16	Hugh Jackman	Male	White	Actor/Actress
17	Isla Fisher	Female	White	Actor/Actress
18	Marilyn Monroe	Female	White	Actor/Actress
19	John Krasinski	Male	White	Actor/Actress
20	John Slattery	Male	White	Actor/Actress
21	Jon Huntsman	Male	White	Politician/Official
22	Katherine Bailess	Female	White	Actor/Actress
23	Keith Lieberthal	Male	White	Politician/Official
24	Kevin Hart	Male	Black	Actor/Actress
25	Kris Allen	Male	White	Musician
26	Logan Marshall-Green	Male	White	Actor/Actress
27	Lonneke Engel	Female	White	Actor/Actress/Model
28	Adam Levine	Male	White	Musician
29	Mario Lopez	Male	White	Host/Media
30	Michelle Obama	Female	Black	Politician/Official
31	Missi Pyle	Female	White	Actor/Actress
32	Naomi Harris	Female	Black	Actor/Actress
33	Natalie Zea	Female	White	Actor/Actress
34	Nathalia Dill	Female	White	Actor/Actress
35	Olivia Palermo	Female	White	Actor/Actress/Model

36	Pat Boone	Male	White	Musician
37	Rachel McAdams	Female	White	Actor/Actress
38	Richard Marx	Male	White	Musician
39	Rodrigo Diaz	Male	White	Actor/Actress
40	Roger Taylor	Male	White	Musician
41	Ron Perlman	Male	White	Actor/Actress
42	Sam Claflin	Male	White	Actor/Actress
43	Samantha Mumba	Female	Black	Musician
44	Shawn Ashmore	Male	White	Actor/Actress
45	Andrea Navedo	Female	White	Actor/Actress
46	Steven Soderbergh	Male	White	Director
47	Tim Gunn	Male	White	Host/Media
48	Treat Williams	Male	White	Actor/Actress
49	Bahar Soomekh	Female	White	Actor/Actress
50	Wentworth Miller	Male	Biracial	Actor/Actress

Note. U.S. targets (n = 50), selected from the CelebA dataset. Race is the CelebA identity annotation supplied with that dataset.

Table S8.2b

Chinese Target Identities

ID	Name (Chinese)	Pinyin	Name (English)	Gender	Occupation
1	任正非	Ren Zhengfei	Ren Zhengfei	Male	Entrepreneur
2	何炅	He Jiong	He Jiong	Male	Host/Media
3	余华	Yu Hua	Yu Hua	Male	Scholar/Writer
4	全红婵	Quan Hongchan	Quan Hongchan	Female	Athlete
5	刘亦菲	Liu Yifei	Crystal Liu	Female	Actor/Actress/Model
6	刘强东	Liu Qiangdong	Richard Liu	Male	Entrepreneur
7	刘翔	Liu Xiang	Liu Xiang	Male	Athlete
8	华春莹	Hua Chunying	Hua Chunying	Female	Politician/Official
9	周迅	Zhou Xun	Zhou Xun	Female	Actor/Actress/Model
10	奚梦瑶	Xi Mengyao	Ming Xi	Female	Actor/Actress/Model
11	姚明	Yao Ming	Yao Ming	Male	Athlete
12	孙俪	Sun Li	Sun Li	Female	Actor/Actress/Model
13	孙杨	Sun Yang	Sun Yang	Male	Athlete
14	孙燕姿	Sun Yanzi	Stefanie Sun	Female	Musician

15	孙颖莎	Sun Yingsha	Sun Yingsha	Female	Athlete
16	宋茜	Song Qian	Victoria Song	Female	Musician
17	屠呦呦	Tu Youyou	Tu Youyou	Female	Scholar/Writer
18	张怡宁	Zhang Yining	Zhang Yining	Female	Athlete
19	成龙	Cheng Long	Jackie Chan	Male	Actor/Actress/Model
20	撒贝宁	Sa Beining	Sa Beining	Male	Host/Media
21	易烊千玺	Yi Yangqianxi	Jackson Yee	Male	Actor/Actress/Model
22	杨幂	Yang Mi	Yang Mi	Female	Actor/Actress/Model
23	杨紫	Yang Zi	Yang Zi	Female	Actor/Actress/Model
24	杨颖	Yang Ying	Angelababy	Female	Actor/Actress/Model
25	林更新	Lin Gengxin	Kenny Lin	Male	Actor/Actress/Model
26	王一博	Wang Yibo	Wang Yibo	Male	Actor/Actress/Model
27	王菲	Wang Fei	Faye Wong	Female	Musician
28	罗翔	Luo Xiang	Luo Xiang	Male	Scholar/Writer
29	苏炳添	Su Bingtian	Su Bingtian	Male	Athlete
30	范冰冰	Fan Bingbing	Fan Bingbing	Female	Actor/Actress/Model
31	莫言	Mo Yan	Mo Yan	Male	Scholar/Writer

32	董卿	Dong Qing	Dong Qing	Female	Host/Media
33	董明珠	Dong Mingzhu	Dong Mingzhu	Female	Entrepreneur
34	贾玲	Jia Ling	Jia Ling	Female	Actor/Actress/Model
35	赵丽颖	Zhao Liying	Zhao Liying	Female	Actor/Actress/Model
36	迪丽热巴	Dilireba	Dilraba Dilmurat	Female	Actor/Actress/Model
37	邓超	Deng Chao	Deng Chao	Male	Actor/Actress/Model
38	那英	Na Ying	Na Ying	Female	Musician
39	郎朗	Lang Lang	Lang Lang	Male	Musician
40	郭晶晶	Guo Jingjing	Guo Jingjing	Female	Athlete
41	金星	Jin Xing	Jin Xing	Female	Host/Media
42	钟南山	Zhong Nanshan	Zhong Nanshan	Male	Scholar/Writer
43	陈奕迅	Chen Yixun	Eason Chan	Male	Musician
44	雷军	Lei Jun	Lei Jun	Male	Entrepreneur
45	韩红	Han Hong	Han Hong	Female	Musician
46	马云	Ma Yun	Jack Ma	Male	Entrepreneur
47	马龙	Ma Long	Ma Long	Male	Athlete
48	魏大勋	Wei Daxun	Wei Daxun	Male	Actor/Actress/Model

49	鹿晗	Lu Han	Luhan	Male	Musician
50	黄晓明	Huang Xiaoming	Huang Xiaoming	Male	Actor/Actress/Model

Note. Chinese targets (n = 50), the UCSB-SZU-Celeb stimulus set assembled for this study. Pinyin is the standard romanisation; the English column gives the name by which the target is most commonly known in English-language sources, which for some targets is a stage name rather than a romanisation. All targets are Chinese nationals and ethnicity was not coded, so no race breakdown is available for this set.

S9. Inter-rater consistency: full results

Table S9

Intraclass Correlation Coefficients for Each Source of Rating Variance

Panel A. U.S. sample

Outcome	ICC_{target}	$ICC_{participant}$	ICC_{module}	$ICC_{residual}$
Trait space	.048	.035	.000	.917
Warm	.161	.105	.000	.734
Critical	.072	.107	.000	.821
Competent	.079	.153	.000	.767
Practical	.064	.099	.000	.836
Feminine	.772	.031	.001	.196
Strong	.240	.134	.000	.626
Youthful	.476	.083	.003	.438
Charismatic	.078	.100	.000	.822

Panel B. Chinese sample

Outcome	ICC_{target}	$ICC_{participant}$	ICC_{module}	$ICC_{residual}$
Trait space	.043	.033	.000	.924
Warm	.108	.108	.000	.784
Critical	.138	.123	.002	.737

Competent	.145	.155	.000	.700
Practical	.158	.128	.000	.715
Feminine	.851	.010	.000	.139
Strong	.350	.120	.000	.531
Youthful	.644	.064	.000	.292
Charismatic	.135	.112	.002	.750
Trustworthy	.099	.148	.001	.752
Attractive	.299	.117	.000	.584

Note. Coefficients come from null multilevel models with random intercepts for target, participant, and image module, fitted separately to each trait and to the pooled multidimensional trait space; each is that source's share of total rating variance. In the trait-space model, trait means are pooled into the residual, so those coefficients are conservative estimates of target-level consensus. The module component is negligible throughout, which is why image module was not carried as a control in the analyses reported in the main text.